



HAL
open science

The influence of cloud chemistry on HO_x and NO_x in the Marine Boundary Layer: a 1-D modelling study

J. E. Williams, F. J. Dentener, A. R. van den Berg

► To cite this version:

J. E. Williams, F. J. Dentener, A. R. van den Berg. The influence of cloud chemistry on HO_x and NO_x in the Marine Boundary Layer: a 1-D modelling study. *Atmospheric Chemistry and Physics Discussions*, 2001, 1 (2), pp.277-335. hal-00300875

HAL Id: hal-00300875

<https://hal.science/hal-00300875>

Submitted on 18 Jun 2008

HAL is a multi-disciplinary open access archive for the deposit and dissemination of scientific research documents, whether they are published or not. The documents may come from teaching and research institutions in France or abroad, or from public or private research centers.

L'archive ouverte pluridisciplinaire **HAL**, est destinée au dépôt et à la diffusion de documents scientifiques de niveau recherche, publiés ou non, émanant des établissements d'enseignement et de recherche français ou étrangers, des laboratoires publics ou privés.

Clouds, HO_x and NO_x
in the MBL

J. E. Williams et al.

The influence of cloud chemistry on HO_x and NO_x in the Marine Boundary Layer: a 1-D modelling study

J. E. Williams^{1,2}, F. J. Dentener³, and A. R. van den Berg¹

¹IMAU, University of Utrecht, Utrecht, The Netherlands

²Current Address: FOM-AMOLF, Kruislaan 107, Amsterdam, The Netherlands

³Joint Research Center, Environment Institute, Ispra(Va), Italy

Received: 6 July 2001 – Accepted: 16 July 2001 – Published: 25 October 2001

Correspondence to: J. E. Williams (williams@amolf.nl)

Title Page

Abstract

Introduction

Conclusions

References

Tables

Figures

◀

▶

◀

▶

Back

Close

Print Version

Interactive Discussion

© EGS 2001

Abstract

A 1-D marine stratocumulus cloud model has been supplemented with a comprehensive and up-to-date aqueous phase chemical mechanism for the purpose of assessing the impact that the presence of clouds and aerosols has on gas phase HO_x , NO_x and O_3 budgets in the marine boundary layer. The simulations presented here indicate that cloud may act as a heterogeneous source of HONO_g via the conversion of $\text{HNO}_{4(g)}$ at moderate pH (~ 4.5). The photolysis of nitrate (NO_3^-) has also been found to contribute to this simulated increase in HONO_g by $\sim 5\%$ and also acts as a minor source of $\text{NO}_{2(g)}$. The effect of introducing deliquescent aerosol on the simulated increase of HONO_g is negligible. The most important consequences of this elevation in HONO_g are that, in the presence of cloud, gas phase concentrations of NO_x species increase by a factor of 2, which minimises the simulated decrease in $\text{O}_{3(g)}$, and results in a regeneration of OH_g . This partly compensates for the removal of OH_g by direct phase transfer into the cloud and has important implications regarding the oxidising capacity of the marine boundary layer. The findings presented here also suggest that previous modelling studies, which neglect the heterogeneous $\text{HNO}_{4(g)}$ reaction cycle, may have over-estimated the role of clouds as a sink for OH_g and $\text{O}_{3(g)}$ in unpolluted oceanic regions, by $\sim 10\%$ and $\sim 2\%$, respectively.

1. Introduction

The Marine Boundary Layer (MBL) may, under many meteorological conditions, be described as a three phase chemical system where species have the potential to interchange between each phase (gas, deliquescent aerosol and cloud) e.g. van den Berg et al. (2000). Aerosol particles are ubiquitous throughout the MBL where they originate from sea spray droplets, which are produced via the mechanical agitation of the ocean's surface by wind and e.g. non-sea-salt sulfate produced from anthropogenic and biogenic DMS and SO_2 . Many of these particles, which reside above the ocean,

Clouds, HO_x and NO_x in the MBL

J. E. Williams et al.

Title Page

Abstract

Introduction

Conclusions

References

Tables

Figures

◀

▶

◀

▶

Back

Close

Print Version

Interactive Discussion

© EGS 2001

**Clouds, HO_x and NO_x
in the MBL**

 J. E. Williams et al.

[Title Page](#)
[Abstract](#)
[Introduction](#)
[Conclusions](#)
[References](#)
[Tables](#)
[Figures](#)
[I◀](#)
[▶I](#)
[◀](#)
[▶](#)
[Back](#)
[Close](#)
[Print Version](#)
[Interactive Discussion](#)

© EGS 2001

are hygroscopic in nature and become deliquescent at relative humidities above 60–70%. Turbulent mixing above the ocean results in the diffusion of the smallest size fraction of these particles ($< 10\mu\text{M}$) throughout the entire MBL. Once such particles enter supersaturated air ($\text{RH} > 100\%$) they may become activated into cloud droplets, thus serving as cloud condensation nuclei (CCN). Although the volume fraction of the aqueous phase is relatively small compared to that of the gas phase, the rates of chemical processes which occur on and in deliquescent aerosol and in cloud droplets can be much faster than the corresponding gas phase processes. Thus, heterogeneous production and loss of key gas phase oxidants may have an appreciable effect on the gas phase composition of the MBL, as demonstrated by a host of previous modelling studies (e.g. Sander and Crutzen, 1996; Liang and Jacobsen, 1999). The magnitude of such influences is principally governed by the extent to which species become partitioned between different phases and their lifetime once incorporated. This, in turn, is determined by physical and chemical characteristics such as the total surface area of particles/droplets, solubility, acidity, reactivity and temperature.

The budget of NO_x (= NO + NO₂) in the MBL is important in determining the concentration of tropospheric pollutants such as O₃. This arises from the complex interactions which exist in the gas phase between HO_x and NO_x species. The most important gas phase reactions are described by reactions (1) – (8)





Moreover, NO_2 , NO_3 , HONO and HNO_4 all photo-dissociate efficiently during daytime, the latter three processes resulting in a regeneration of NO_x .

Both NO and NO_2 are themselves relatively insoluble ($K_H = 1.2 \times 10^{-2} \text{ M atm}^{-1}$ for both) meaning that removal of NO_x by phase transfer on both deliquescent aerosol and cloud droplets is rather limited. However, the loss of NO_x reservoir species (e.g. HNO_3 , NO_3^- and N_2O_5) by heterogeneous removal routes has been the subject of a host of recent laboratory studies (e.g. Fenter et al., 1996; Behnke et al., 1997; Schweitzer et al., 1998; Davies and Cox, 1998) which have concluded that the heterogeneous conversion of NO_x to NO_3^- is relatively efficient under typical atmospheric conditions. Moreover, global modelling studies also suggest that such heterogeneous loss processes are fairly efficient pathways for removing NO_x from the atmosphere via aggregation/deposition (e.g. Dentener and Crutzen, 1993; Lawrence and Crutzen, 1998). Once formed in the aqueous phase, NO_3^- is fairly stable and for it to be re-oxidised into NO_x would require the presence of an extremely strong oxidising agent such as F_2 (Ravishankara and Longfellow, 1999). However, laboratory measurements suggest that the photolysis of NO_3^- in solution may also occur, resulting in a substantial regeneration of NO_2 (Zellner et al., 1990), R9, which could either react further or escape back into the gas phase:



One of the major uncertainties in the current knowledge related to nitrogen containing species in the troposphere is the mechanism by which the accumulation of HONO_g (nitrous acid) occurs during the night (Jacob, 2000). The photolysis of HONO_g is relatively efficient, and is considered to be an important early morning source of OH_g in high NO_x environments, such as urban centres (Harrison et al., 1996), where typical mixing ratios for HONO_g can reach several nmol/mol by the end of the night (Calvert

**Clouds, HO_x and NO_x
in the MBL**J. E. Williams et al.

Title Page

Abstract

Introduction

Conclusions

References

Tables

Figures

◀

▶

◀

▶

Back

Close

Print Version

Interactive Discussion

© EGS 2001

**Clouds, HO_x and NO_x
in the MBL**

 J. E. Williams et al.

[Title Page](#)
[Abstract](#)
[Introduction](#)
[Conclusions](#)
[References](#)
[Tables](#)
[Figures](#)
[I◀](#)
[▶I](#)
[◀](#)
[▶](#)
[Back](#)
[Close](#)
[Print Version](#)
[Interactive Discussion](#)

© EGS 2001

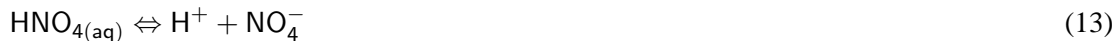
et al., 1994). Recently, measurements performed at both a coastal site (Grenfell et al., 1999) and in the free troposphere (Jaegle et al., 1999) also suggest that the photodissociation of HONO_g produces significant amounts of [OH_g] at sunrise. However, the gas phase production of HONO, R3, is small during the night and the existence of an additional source of HONO_g is needed which is efficient at this time. Certain authors have suggested that heterogeneous surfaces may act as sites for NO_x conversion (Bambauer et al., 1994; Harrison and Collins, 1998; Kleffmann et al., 1999), vis;



However, the reaction probability (γ) of NO₂ is rather uncertain (with values ranging from between 10⁻³–10⁻⁶). Thus, in the latter case this route may not be of any significant importance to the overall NO_x budget. The lack of any substantiated heterogeneous conversion pathway has provided the impetus for the recent intensity in laboratory investigations concerned with the effects that surfaces, (e.g. soot) may have on the conversion of NO₂ to HONO (e.g. Gerecke et al., 1998; Longfellow et al., 1999; Kalberer et al., 1999). However, in most cases in the MBL, the concentrations of such particles are thought to be relatively low (e.g. Cooke et al., 1997). Therefore, for heterogeneous HONO formation to occur in remote marine locations another pathway would be needed.

In this paper we focus on the effect that the in situ production of HONO_{aq} within cloud droplets and aerosol may have on levels of HONO_g present in the MBL. This paper was partly motivated by the work of Dentener et al. (2001) and Warneck (1999) who have suggested that the aqueous phase reaction of HNO₄ exerts a significant influence on tropospheric chemistry. The mechanism by which such a conversion could occur involves the uptake and subsequent dissociation of HNO₄ (pK_a = 5), an important reservoir species for NO₂ in the gas phase (equilibrium (7)). The K_H (HNO₄) is relatively high ($\sim 10^4$ M atm⁻¹ at 298 K), with the uptake, equilibrium (12), being enhanced

due to the dissociation of HNO_4 to its associated anion, NO_4^- , once incorporated into solution, equilibrium (13);



5 Moreover $\text{HNO}_{4(\text{aq})}$ may be formed in situ via equilibrium (14), although this route may only be important if there is an efficient in situ source of $\text{NO}_{2(\text{aq})}$, i.e. the reaction is not limited by the low value of $K_H(\text{NO}_2)$;



10 Furthermore, NO_4^- undergoes a relatively slow (0.8 s^{-1}) unimolecular decomposition to form the NO_2^- anion, R15:



If the solution is sufficiently acidic ($\text{pH} < 4$) protonation of NO_2^- occurs forming HONO ($\text{pK}_a = 3.3$), equilibrium (16), which may then be transferred back into the gas phase, equilibrium (17), where it has the potential to regenerate NO_g :



20 This reaction sequence is important since it provides a pathway for the net reduction of $\text{HO}_{2(\text{g})}$ to OH_g , without oxidising CO_g , and $\text{NO}_{2(\text{g})}$ to NO_g , without producing $\text{O}_{3(\text{g})}$. However, due to the overall cycle being pH limited, this mechanism will only be important in dilute solution, i.e. the low pH commonly associated with deliquescent aerosol will hinder the dissociation of $\text{HNO}_{4(\text{aq})}$. Therefore, under the relatively unpolluted conditions typical of the MBL, this heterogeneous process could have important implications to the budget of NO_x , which also affects the budget of $\text{O}_{3(\text{g})}$, the photolytic pre-cursor for OH_g .

Title Page

Abstract

Introduction

Conclusions

References

Tables

Figures

◀

▶

◀

▶

Back

Close

Print Version

Interactive Discussion

In clear air the major production route for $O_{3(g)}$ is R6, followed by the photo-dissociation of $NO_{2(g)}$, R18.



However, in the presence of cloud, the depletion of $HO_{2(g)}$ by phase transfer suppresses R6 therefore reducing the overall rate of $O_{3(g)}$ formation. By introducing a heterogeneous feedback mechanism that elevates $[NO_g]$ in interstitial air, such as that suggested here, this reduction could be offset to a certain extent. Moreover, the release of $HONO_g$, via R17, could also offset the depletion of OH_g in cloud. This could also exert an additional influence on the $O_{3(g)}$ budget by increasing both $[HO_{2(g)}]$ and $[RO_{2(g)}]$ via the oxidation of CO_g and $CH_{4(g)}$, respectively. Once present, $RO_{2(g)}$ may produce $NO_{2(g)}$ via R19:



As explained earlier, previous modelling studies have focused on the role clouds and aerosol play with respect to sulphur chemistry (Warneck, 1999; O'Dowd et al., 2000), halon chemistry (Sander and Crutzen, 1996), ozone and free-radicals (Lelieveld and Crutzen, 1991; Walcek et al., 1997; Herrmann et al., 2000b). Here we expand on these earlier studies and present the results of a 1-D modelling study whose aim is to investigate whether the presence of cloud substantially modifies the resident concentrations of HO_x ($= OH + HO_2$) and NO_x ($= NO + NO_2$) in the marine boundary layer when accounting for the heterogeneous reduction of HNO_4 to $HONO$. In the following section we briefly describe the 1-D stratocumulus cloud model used for performing the simulations presented here. Thereafter, we discuss the results of both a binary (gas and cloud) and tertiary (gas, aerosol and cloud) phase run and compare them to a base simulation that neglects heterogeneous interactions. Then we present the results of some sensitivity runs whose purpose is to differentiate which processes in the proposed conversion mechanism have the largest impact on the simulated effects on HO_x and NO_x . Finally, we discuss the uncertainties present in the model and then summarise with conclusions related to the effect of cloud on the HO_x and NO_x budget.

**Clouds, HO_x and NO_x
in the MBL**J. E. Williams et al.

[Title Page](#)[Abstract](#)[Introduction](#)[Conclusions](#)[References](#)[Tables](#)[Figures](#)[I◀](#)[▶I](#)[◀](#)[▶](#)[Back](#)[Close](#)[Print Version](#)[Interactive Discussion](#)

© EGS 2001

2. Model description

2.1. Details of the model

The 1-D chemistry transport model used in this study has recently been published by van den Berg et al. (2000), where the focus was on the sulphur cycle in the MBL. Therefore only a short summary will be given here. The model is a 21-layer one-dimensional (column) model and consists of a meteorological, microphysical and a chemistry-transport module.

An existing meteorological model for the marine boundary layer of Duynkerke and Driedonks (1987) was used which includes prognostic equations for the horizontal velocities, the wet equivalent potential temperature and total water content. Together with the prescribed boundary conditions (e.g. roughness length, surface temperature) these equations determine the temperature and humidity, turbulent mixing, condensation/evaporation of cloud water, radiative heating/cooling and sensible heat fluxes in the boundary layer.

The microphysical module describes the number and mass distribution functions of aerosol particles and cloud droplets and the change in these size distributions due to microphysical processes. The aerosol population is represented by several different types of particle (e.g. NH_4HSO_4 , $(\text{NH}_4)_2\text{SO}_4$ and NaCl), where each type is represented by one, two or three (overlapping) log-normal modes. By assuming that aerosol particles are in equilibrium with the ambient relative humidity, the size of the wet aerosol particles is related to their dry size by the empirical relationship of Fitzgerald (1975). At a relative humidity $> 80\%$ all aerosol particles are deliquescent and have an associated water content. Cloud liquid water is distributed over droplet sizes according to a Γ distribution (Roger and Yau, 1994). The parameters for this function are determined by the cloud liquid water content and the amount of activated aerosol particles, where the liquid water content is calculated by the meteorological module. The amount of activated aerosol particles is calculated following the parameterization of Flossmann et al. (1985). A schematic representation of the overall model is shown in Fig. 1. It is

Title Page

Abstract

Introduction

Conclusions

References

Tables

Figures

◀

▶

◀

▶

Back

Close

Print Version

Interactive Discussion

important to note that cloud droplets nucleated on e.g. sea-salt or sulphate, retain their chemical identity, therefore allowing for size resolved chemistry.

The chemistry-transport module describes the emission/dry deposition fluxes, vertical transport by turbulence, exchange between the gas and aqueous phase, the chemical processes in each phase and the chemical processes at the surface of the aqueous and solid phases. Sea-salt emissions are calculated following Monahan et al. (1986) and are a strong function of the wind speed. Adjustments to this approach were made to account for the generation of fine sea-salt particles and are based on the log-linear regression fits for sea salt particles as a function of wind speed according to O'Dowd and Smith (1993). Vertical turbulent transport is parameterized using the turbulent diffusion coefficient for heat and water vapour taken from the meteorological model and the concentration gradient. Aqueous phase chemical species are only allowed to be transported in cloud layers or layers where the relative humidity $> 80\%$. Upon being transported into a layer which has a relative humidity $< 80\%$ the volatile species are released back into the gas phase. In this work we used first-order deposition velocities to describe all dry deposition fluxes, since for most species the parameters needed to calculate the resistance fluxes were not available and a more detailed approach does not seem necessary for this particular model study.

The formation of stratocumulus clouds requires both stable stratification in the free troposphere above the boundary layer (i.e. no deep convection) and a sufficient supply of moisture into the boundary layer. Such conditions are commonly found in the MBL at mid-latitudes during the summertime. Once formed, stratocumulus cloud decks persist for a long time providing an ideal scenario under which to investigate the impact of clouds on the regional climate. For this reason we chose our meteorological conditions to be representative of such a location, i.e. the Atlantic Ocean off the coast of Spain (45°N). Moreover, our main focus was to investigate the effect of cloud over a number of consecutive days rather than just a few hours, which requires relatively stable boundary conditions to prevent cloud dissipation.

**Clouds, HO_x and NO_x
in the MBL**J. E. Williams et al.

[Title Page](#)[Abstract](#)[Introduction](#)[Conclusions](#)[References](#)[Tables](#)[Figures](#)[I◀](#)[▶I](#)[◀](#)[▶](#)[Back](#)[Close](#)[Print Version](#)[Interactive Discussion](#)

© EGS 2001

2.2. Chemistry of the model

2.2.1. Gas phase chemistry

A complete listing of the chemical species included within the gas-, aerosol- and aqueous-phases in the 1-D model is given in Table 1. Here, the most important sulphur, nitrogen, carbon, HO_x, chlorine and bromine compounds are all accounted for making the overall chemistry fairly comprehensive.

The gas-phase chemistry is described by using the RACM chemical mechanism of Stockwell et al. (1997) and was chosen since it is a versatile yet condensed mechanism which includes a detailed description of the most important organic reactions as well as a realistic production of NO_x. As RACM does not contain any gas phase chemistry of reactive halogen species, nor the oxidation of dimethyl sulphide (DMS), the existing scheme was supplemented with 11 additional photolysis reactions and 46 gas-phase reactions, which are listed in Tables 2 and 3, respectively. The photolysis rates are parameterised following the approach of Krol and van Weele (1997) and Landgraf and Crutzen (1998). For the lumped species used by RACM, which account for the behaviour of higher hydrocarbons, this approach is not directly applicable (e.g. DIEN or HKET) so the photolysis rates for such species were scaled to other species exhibiting similar photolysis absorption spectra as described in Table 2. Irreversible heterogeneous uptake on aerosol particles and cloud droplets was included for ClNO₂, BrNO₂ and H₂SO₄ following the approach of Sander and Crutzen (1996). The phase transfer of chemical species between the gas phase and the wet aerosol/cloud droplets was calculated using the method of Schwartz (1986). The values for the Henry's constants (K_H), gas phase diffusion coefficients (D_g) and accommodation co-efficients (α) were taken directly from Herrmann et al. (2000b), except for the organic peroxy-radicals. For certain lumped species used in RACM simplifications were made regarding their chemical state once transferred into the liquid phase, e.g. ORA2 is transferred in solution as CH₃COOH.

Clouds, HO_x and NO_x in the MBL

J. E. Williams et al.

Title Page

Abstract

Introduction

Conclusions

References

Tables

Figures

◀

▶

◀

▶

Back

Close

Print Version

Interactive Discussion

© EGS 2001

2.2.2. Aqueous phase chemistry

The aqueous phase chemistry was described by using a reaction mechanism (CAPRAM 2.4) that incorporates a full description of C_1 and C_2 chemistry. The mechanism was constructed in collaboration with several groups (Herrmann et al., 2000b). It evaluates and utilises the most recent laboratory data to produce an up-to-date reaction mechanism suited for describing the chemistry which occurs on deliquescent aerosol and in cloud droplets. Due to the size of this mechanism (86 species, 178 reactions) it is not reproduced here, although it is available as an electronic supplement to this paper. In this study the mechanism was used for the reactions which occur both in aerosol associated water and cloud droplets. However, due to the limited data available concerning activity co-efficients for the chemical species declared in CAPRAM 2.4, no corrections were made to the rates of reaction used in the deliquescent aerosol compared to those used for dilute solution. As CAPRAM 2.4 was designed for a more general application than simulating the chemistry that occurs in the MBL, several modifications were made. These modifications were mainly made to improve both model stability and expand the number of reactions involving reactive halogen species. The modifications are: (i) no explicit formation of peroxy radicals, i.e. the reaction of free-radical species with $O_{2(aq)}$ was considered to be so fast as to be instantaneous on the time scale of the simulations, (ii) phase exchange was included for HBr, BrOH, ClOH, and $H_2C_2O_4$ using the values given in Table 4, (iii) 26 additional aqueous phase reactions were included to account for the formation of volatile halogen species in solution, see Table 5, (iv) the Henry's constants for CH_3O_2 and $CH_3CH_2O_2$ were scaled to those of CH_3OOH and CH_3CH_2OOH , respectively, using the ratio $K_H(HO_2)/K_H(H_2O_2)$, as suggested by Liang and Jacob (1997), (v) the uptake of $H_2C_2O_4$, formation of hydroxymethanesulphanoate (HMS^-) and the reactions of copper were not incorporated into the aerosol chemistry due to computational limitations, (vi) the equilibrium constant for CO_2 was described using a single equilibrium step (Lelieveld and Crutzen, 1991) (vii) the reaction of HNO_4 with HSO_3^- replaced the reaction of $HONO_{aq}$ with OH_{aq} (see elec-

Title Page

Abstract

Introduction

Conclusions

References

Tables

Figures

◀

▶

◀

▶

Back

Close

Print Version

Interactive Discussion

© EGS 2001

tronic supplement) and (viii) the rate of R14 and the mechanism for the formation of HMS^- in dilute solution were taken from Warneck (1999). Model runs were performed for a mid-latitude of 45°N over a period of five days, starting at midnight on 21 June, since we expect the maximal effect on photochemistry to occur under these conditions.

5 Although other locations and seasons may also be interesting, the number of simulations is limited for computational reasons, i.e. a 5 day coupled gas-cloud-aerosol run takes over 48 hours processor time on a UNIX workstation. The initial conditions were chosen to be representative of an air-mass that is influenced by continental emissions and subsequently advected over the ocean, see Table 6. At the start of each simulation
10 all gas phase species were assumed to be homogeneously distributed across the entire height of the 1-D model, i.e. the first 2 km. The emission fluxes and deposition velocities used throughout the simulations were prescribed using the values given in Tables 7 and 8, respectively, and represent the release/loss of gaseous species from/to the oceans surface.

15 3. Model results

In Fig. 2 we show the development of the cloud layer during a typical simulation using our 1-D model. The cloud layer forms during the first two hours of the simulation and persists for the entire duration of the run, over which time it develops according to changes in the meteorological conditions, e.g leading to increases in the boundary
20 layer height. It can be clearly seen that the depth of the cloud layer increases to approximately 500 m by the fifth day whilst the cloud base increases from 400 to 600 m. The liquid water content within the cloud layer was limited to 1 g cm^{-3} and the mean radius of the droplets was 7 μm , which is thought to be representative of non-precipitating conditions.

25 In the following sections we present the results obtained when introducing cloud and aerosol/cloud interactions into the model and compare them with a reference simulation which accounts for gas phase processes only. Comparisons are made for the fifth

Title Page

Abstract

Introduction

Conclusions

References

Tables

Figures

◀

▶

◀

▶

Back

Close

Print Version

Interactive Discussion

**Clouds, HO_x and NO_x
in the MBL**J. E. Williams et al.

[Title Page](#)[Abstract](#)[Introduction](#)[Conclusions](#)[References](#)[Tables](#)[Figures](#)[I◀](#)[▶I](#)[◀](#)[▶](#)[Back](#)[Close](#)[Print Version](#)[Interactive Discussion](#)

© EGS 2001

day of each simulation over a 12 hour period (between 6 am and 6 pm). After 5 days the simulation is not influenced by the initial conditions whereas the chemical regime remains rather similar. Each comparison is segregated into three distinct height regimes which were chosen to emphasise the differences that occur below the cloud (< 600 m), in the cloud (600–1520 m) and above the cloud (> 1520 m) being representative of the lower free troposphere. All the different cases considered in this study are defined in Table 9. Reference case (I) is simply a clear sky gas phase simulation. Case (II) is similar to case (I) except that the attenuation of photolysing light by the cloud layer is still accounted for to allow differentiation between radiative and chemical effects introduced due to the presence of cloud. All other cases include heterogeneous interactions, including the attenuation of photolysis rates by cloud, where case (III) considers a binary phase chemical system (gas and cloud only) and case (IV) considers a tertiary phase chemical system (gas, aerosol and cloud) using the CAPRAM 2.4 scheme described above. For the binary phase chemical system a number of sensitivity runs were performed to establish the importance of certain chemical processes to the overall effect of cloud simulated by the model. Case (V) ignores the phase transfer of both HONO_g and HNO_{4(g)} and also the insitu formation of HNO_{4(aq)} by equilibrium (13). Case (VI) ignores NO₃⁻ photolysis in the aqueous phase, so as to limit in situ NO_{2(aq)} production, and investigates the contribution of this process to HONO formation. Finally, case (VII) investigates the importance of the additional halogen chemistry to the simulated perturbation in O_{3(g)} at this summer mid-latitude location.

3.1. Influence of cloud

The effect of introducing cloud and aerosol into our model simulations (i.e. cases (III) and (IV)) on the gas phase concentrations of O₃, HO_x and NO_x species are summarised in Tables 10a and 10b, respectively. Here ratios are given relative to reference case (I), as well as case (II), with the latter emphasising the effects of chemistry only. By comparing the ratios for a chosen species and height regime it can be seen that the ‘clear sky’ ratios are quite different to the corresponding ‘attenuated’ ratios for both

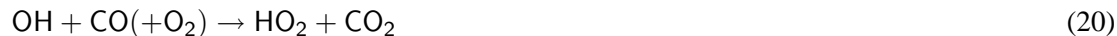
**Clouds, HO_x and NO_x
in the MBL**

 J. E. Williams et al.

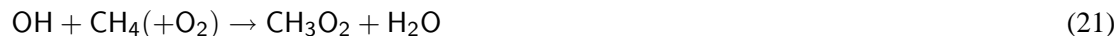
[Title Page](#)
[Abstract](#)
[Introduction](#)
[Conclusions](#)
[References](#)
[Tables](#)
[Figures](#)
[I◀](#)
[▶I](#)
[◀](#)
[▶](#)
[Back](#)
[Close](#)
[Print Version](#)
[Interactive Discussion](#)

© EGS 2001

cases (III) and (IV). For the cloud only run, case (III), Figs. 3a and b show that during the first 3 days, at a height of ~ 1060 m, i.e. just above the cloud top, the $[\text{HO}_2]_{\text{g}}$ level increases by more than a factor of 2 due to the significant back-scattering of the photolytic radiation (after the third day the air is within the cloud). Under the relatively clean conditions of our simulations, i.e. low NO_x and VOC, this increase during the first days is principally due to the enhanced photo-dissociation of $\text{O}_3(\text{g})$. This subsequently increases the rate of OH_{g} production and leads to associated increases in $[\text{HO}_2]_{\text{g}}$ by R20, which is considered to be the major gas phase sink for OH_{g} ;



Moreover, there is also a positive feedback effect due to an increase in the rate of R6, which recycles OH_{g} . This is confirmed by the profiles of $\text{HO}_x(\text{g})$ below the cloud layer at ~ 500 m (Figs. 4a and b). At this height, diffusion of the light through the cloud deck subdues the photochemical formation of OH_{g} which subsequently suppresses $\text{HO}_2(\text{g})$ production and the efficiency of R6, i.e. less OH_{g} is recycled. The second most important gas phase sink for OH_{g} is the oxidation of $\text{CH}_4(\text{g})$, R21;



This results in a $\sim 40\%$ increase in the resident $[\text{CH}_3\text{O}_2]_{\text{g}}$ at ~ 1060 m compared to case (I) (not shown). The predominant removal pathway for $\text{CH}_3\text{O}_2(\text{g})$ in relatively unpolluted air, i.e. low NO_x , is its termination involving $\text{HO}_2(\text{g})$, R22, which results in a 0.1 nmol/mol increase in $\text{CH}_3\text{OOH}(\text{g})$ by the third day for case (III) at ~ 1060 m (not shown);



After the third day, at our chosen height of analysis of 1060 m, the cloud layer develops to such an extent that during the fourth and fifth day the air resides ‘in-cloud’ (Fig. 2). Once this transition occurs a rapid depletion of $[\text{HO}_2]_{\text{g}}$ is observed. This is due to the efficient uptake of HO_x within the cloud droplets, where the fast destruction of OH_{aq} by the reaction with solutes, such as the formate ion (HCOO^-) and hydrated

formaldehyde ($\text{CH}_2(\text{OH})_2$), means that the droplets act as an efficient sink for OH_g . The uptake of $\text{HO}_2(\text{g})$ is even more efficient than for OH_g , due to its relatively high solubility ($K_H = 9 \times 10^3 \text{ M atm}^{-1}$ at 298 K) and its dissociation in mildly acidic solution ($\text{pH} > 4$), equilibrium (23), which effectively increases the amount transferred into solution;



Both of these findings agree with of a host of previous box-modelling studies conducted to investigate the effect of clouds on HO_x and O_3 formation (e.g. Lelieveld and Crutzen, 1991; Matthijsen et al., 1995; Walcek et al., 1997) and have been discussed at length in these articles. Therefore, since our work confirms previous studies, no further discussion concerning the fate of these radicals in the condensed phase is included here.

The situation for NO_x is somewhat more complicated as the amount removed from the gas phase by direct phase transfer is limited by low solubility (Schwartz and White, 1983). Figure 3d shows that there is a decrease in $[\text{NO}_2]_g$ above the cloud top by 20% during the first three days of the simulation. There is also a corresponding increase for $[\text{NO}]_g$ which is principally due to an increase in the photolysis rate of $\text{NO}_2(\text{g})$, R18. Therefore, even though recycling of $\text{NO}_2(\text{g})$ (via R6) will increase due to the simultaneous elevation in $[\text{HO}_2]_g$ (Fig. 3b) this process does not compensate for the enhanced photochemical destruction of $\text{NO}_2(\text{g})$ via R18. Once the air moves into the cloud layer the $[\text{NO}_2]_g$ increases by $\sim 30\%$ during the fifth day, which rises to $\sim 50\%$ during the fifth night (Fig. 3d). For $(\text{NO})_g$ there is also a simultaneous increase at 1060 m, as a result of heterogeneous conversion of NO_2 (Fig. 3c). The reasons for this are discussed in more detail below in the section concerned with the sensitivity studies. Below the cloud deck, at $\sim 500 \text{ m}$ (Figs. 4c and d), the $[\text{NO}_2]_g$ increases from between 10–30 pmol/mol on the fifth day due to a reduction in the intensity of photolysing light. An associated decrease in $[\text{NO}]_g$ also occurs at this level although the regeneration of NO_g via heterogeneous routes limits this decrease to between 1–2 pmol/mol.

The fluctuation of gas phase $[\text{HO}_x]$ and $[\text{NO}_x]$ due to heterogeneous effects means that the chemical lifetime of $[\text{HNO}_4]_g$ is also affected by the presence of cloud (Table

**Clouds, HO_x and NO_x
in the MBL**J. E. Williams et al.

Title Page

Abstract

Introduction

Conclusions

References

Tables

Figures

I◀

▶I

◀

▶

Back

Close

Print Version

Interactive Discussion

© EGS 2001

**Clouds, HO_x and NO_x
in the MBL**J. E. Williams et al.

10a). Thus, a concentration ratio of 1.65 is obtained at ~ 500 m which is directly associated with the increase in $[\text{NO}_2]_{\text{g}}$ (the $[\text{HO}_2]_{\text{g}}$ ratio being almost unity). However, it must be noted that the magnitude of these increases are quite different ($[\text{HNO}_4]_{\text{g}} \sim 0.5$ pmol/mol, $[\text{NO}_2]_{\text{g}} \sim 5$ pmol/mol). In the cloud layer HNO_4 decreases of $\sim 20\%$ are predicted due to both direct phase transfer, equilibrium (12), and the depletion of $[\text{HO}_2]_{\text{g}}$, which alters the equilibrium position of (7), (see discussion below for case (V)). Above the cloud (> 1520 m) no differences in $[\text{HNO}_4]_{\text{g}}$ occur, when using case (II) as the reference case, due to the fact that no substantial detrainment of NO_x from the cloud layer occurs. An additional reservoir species for $\text{NO}_{2(\text{g})}$ which is accounted for in the RACM mechanism is peroxyacetylnitrate (PAN), equilibrium (24);



For cases (I) and (III) typical concentrations of PAN formed during the first day of the simulation range from between 30–40 nmol/mol (not shown), which persists for the entire simulation. However, PAN_{g} simply acts as a reservoir for $\text{NO}_{2(\text{g})}$ and no heterogeneous removal of nitrogen occurs by the phase transfer of this species (McFadyen and Cape, 1999). For this reason not further analysis of PAN_{g} is performed in this paper.

The strongest effect on nitrogen containing species is the large increase in $[\text{HONO}]_{\text{g}}$, which is computed to occur over the 5 days of simulation. Figure 5a compares the $[\text{HONO}]_{\text{g}}$ profiles at 1060 m for cases (II) and (III). Here it can be clearly seen that between 2–10 nmol/mol of HONO_{g} accumulates at this level over the course of a night, which subsequently photolyses at dawn. The reaction sequence, which is thought to be the dominant pathway for this reduction of $\text{NO}_{2(\text{g})}$ to NO_{g} , is R7–R12–R13–R15–R16–R17 (see sensitivity studies below). The efficiency of this mechanism depends critically on the pH of the cloud due to equilibria (13) and (16) being protonation steps. In our simulations the pH inside the droplets is ~ 4.5 (not shown), which is typical of relatively unpolluted conditions, such as those chosen for these model runs, and is mainly governed by the availability of inorganic acids, namely $\text{H}_2\text{SO}_{4(\text{g})}$, $\text{HNO}_{3(\text{g})}$ and

[Title Page](#)[Abstract](#)[Introduction](#)[Conclusions](#)[References](#)[Tables](#)[Figures](#)[I◀](#)[▶I](#)[◀](#)[▶](#)[Back](#)[Close](#)[Print Version](#)[Interactive Discussion](#)

© EGS 2001

**Clouds, HO_x and NO_x
in the MBL**J. E. Williams et al.

HCl_(g). This pH value is fortuitous in that the HNO_{4(aq)}: NO₄⁻ and HONO_(aq): NO₂⁻ ratios are (0.60 : 0.40) and (0.05 : 0.95), respectively, which allows the formation of HONO_(aq) to occur, a certain fraction of which then escapes back into the gas phase. The main consequence of this process is to enhance the resident [NO]_g and [OH]_g present during the course of the day compared with a simulation which neglects the heterogeneous release of HONO_g, i.e. case (V). The implications of this are discussed in detail in the preceding section.

3.2. Influence of aerosol

Figures 3 and 4 also show profiles for the cloud plus aerosol run (case IV) at 1060 m and ~ 500 m, respectively. From these profiles it can be seen that the general trends for HO_x and NO_x are very similar to the cloud only runs (case III). Therefore, for brevity, only the differences between cases (III) and (IV) will be discussed here. The budget of OH_g is affected somewhat more at the lower level (~ 10% under the cloud) than at the higher level (~ 2% at the cloud-top) due to the introduction of deliquescent aerosol (Figs. 3a and 4a, respectively, and Table 10b). These differences maybe explained by considering the ratios of other reactive gases at these respective heights. This perturbation in OH_g is an indirect effect of the ~ 2% decrease in O_{3(g)} between cases (III) and (IV), which is predominantly due to an increase in reactive bromine species released from the aerosol and the associated destruction via reaction G(16), Table 3. The aerosol particles themselves act as negligible sinks for OH_g compared to cloud droplets since at the low aerosol water pH the speciation of the dissociating solutes does not promote reactions of OH_{aq}. For HO_{2(g)} slight increases are simulated at both heights compared with case (III), with the most marked effect being near the cloud top (~ 1060 m, Fig. 4b). No significant uptake of HO_{2(g)} occurs on the aerosol due to the low pH of the associated water limiting the dissociation via equilibrium (23). Therefore, this simulated increase is principally due to a change in the gas phase production/destruction of HO_{2(g)}. Again, this maybe explained by considering halogen release from deliquescent aerosol particles which leads to the formation of HO_{2(g)} via

[Title Page](#)[Abstract](#)[Introduction](#)[Conclusions](#)[References](#)[Tables](#)[Figures](#)[I◀](#)[▶I](#)[◀](#)[▶](#)[Back](#)[Close](#)[Print Version](#)[Interactive Discussion](#)

© EGS 2001

G(17) (Table 3), with an associated decrease in $[\text{CH}_2\text{O}_g]$ by $\sim 10\%$ (not shown).

For NO_x species the differences between cases (III) and (IV) are, again, rather small. After initialisation of the model, i.e. excluding the first day, the influence of deliquescent aerosol on $[\text{NO}_{2(g)}]$ leads to a reduction in the mixing ratio by $\sim 2\text{--}3$ nmol/mol at both heights over the fourth and fifth days (Figs. 3d and 4d, respectively). As the intensity of photolysing light is equal between cases (III) and (IV), this difference in $\text{NO}_{2(g)}$ is principally due to the enhanced gas phase formation of species such as $\text{BrNO}_{3(g)}$, via reaction G(20) (Table 3). After formation, $\text{BrNO}_{3(g)}$ may be removed via the irreversible uptake on wetted aerosol surfaces, which removes NO_2 from the gas phase. For $[\text{NO}_g]$ the only discernible differences occur above the cloud deck (compare Figs. 3c and 4c), where there is a reduction in the mixing ratio of $\sim 1\text{--}2$ nmol/mol. This is most probably associated with the decrease in $[\text{NO}_{2(g)}]$, i.e. R18, at this level rather than a direct influence of reactive halogen species. In terms of heterogeneous HONO_g formation the consideration of deliquescent aerosol does not affect the simulated release from the cloud droplets. There is a small indirect effect due to the increase in $[\text{HO}_{2(g)}]$, i.e. $[\text{HNO}_{4(g)}]$ increases marginally (not shown). However, the high acidity of the aerosol associated water does not allow an appreciable dissociation of either HNO_4 or HONO . Therefore, no conversion of NO_2 to NO occurs on the deliquescent aerosol introduced into the model in case (IV).

4. Sensitivity studies

In Figs. 5 to 7 we present the concentration profiles at 1060 m for HONO_g , NO_g and $\text{NO}_{2(g)}$, respectively, for cases (III), (V) and (VI) (Table 9). All comparisons used case (II) as the reference case to highlight the chemical effects of the system and exclude photolytic effects. Three sensitivity runs are discussed here and were specifically chosen to investigate some aspect of the conversion of NO_2 to NO in cloud droplets via the $\text{HNO}_{4(g)}$ reaction sequence. As shown above, aerosol chemistry does not play any significant role in the production of HONO via the reduction of HNO_4 and is not discussed

Title Page

Abstract

Introduction

Conclusions

References

Tables

Figures

◀

▶

◀

▶

Back

Close

Print Version

Interactive Discussion

in these sensitivity studies.

4.1. The effect of $\text{HNO}_{4(\text{g})}$ and $\text{HONO}_{(\text{g})}$ uptake on $\text{HO}_{\text{x}(\text{g})}$ and $\text{NO}_{\text{x}(\text{g})}$

Case (V), which neglects the uptake of $\text{HNO}_{4(\text{g})}$, is presented to substantiate that R12 is the principle route responsible for the simulated release of HONO_{g} as predicted by our model. In addition to neglecting the uptake of $\text{HNO}_{4(\text{g})}$, the in situ formation of $\text{HNO}_{4(\text{aq})}$, equilibrium (14), was also set to zero. The ratios for the gas phase HO_{x} and NO_{x} species, compared with reference case (I), are summarised in Table 11. By comparing the ratios for HONO_{g} with those presented for a standard cloud run (case (III), Table 10a) it can be clearly seen that no significant increase in HONO_{g} occurs for case (V). This corroborates the hypothesis that the heterogeneous reduction of $\text{HNO}_{4(\text{aq})}$ is a key step in the production of HONO_{g} . The most important consequence of this is that both $[\text{NO}_{\text{g}}]$ and $[\text{NO}_{2(\text{g})}]$ decrease by $\sim 50\%$ and $\sim 35\%$, respectively, for case (V) compared to case (III). This has significant implications regarding the net production of $\text{O}_{3(\text{g})}$, which is principally governed by the NO_{g} mixing ratio (Crutzen, 1995). Moreover, the depletion of $[\text{OH}_{\text{g}}]$ simulated for case (V), due to both phase transfer into the cloud and the lower effective rate of R6 seems to be somewhat compensated for in case (III) by the increase in the photolysis of the HONO_{g} , and the elevated $[\text{NO}_{\text{g}}]$, respectively. This suggests that using an aqueous phase mechanism which ignores the reduction of $\text{HNO}_{4(\text{aq})}$ could lead to an overestimation of the effects of cloud on both their efficiency as an OH_{g} sink and their influence on the overall O_3 budget, as can be seen by comparison of the ratios in Tables 10a and 11. A further interesting result is that, even when R12 is neglected, $[\text{HNO}_{4(\text{g})}]$ still decreases by $\sim 55\%$ (Table 11). This is due to the efficiency with which $\text{HO}_{2(\text{g})}$ is depleted from the gas phase, which forces equilibrium (13) towards the left, i.e precipitates the decomposition of $\text{HNO}_{4(\text{g})}$. Comparing the ratio of $\text{HNO}_{4(\text{g})}$ for case (III) with case (II) ($\sim 21\%$ depletion, Table 10a) reveals that the increase in $\text{NO}_{2(\text{g})}$ simulated for case (III) hinders the decomposition of $\text{HNO}_{4(\text{g})}$ compared with a run which ignores the aqueous phase chemistry of HNO_4 (case V).

Clouds, HO_{x} and NO_{x} in the MBL

J. E. Williams et al.

Title Page

Abstract

Introduction

Conclusions

References

Tables

Figures

◀

▶

◀

▶

Back

Close

Print Version

Interactive Discussion

© EGS 2001

**Clouds, HO_x and NO_x
in the MBL**

 J. E. Williams et al.

[Title Page](#)
[Abstract](#)
[Introduction](#)
[Conclusions](#)
[References](#)
[Tables](#)
[Figures](#)
[I◀](#)
[▶I](#)
[◀](#)
[▶](#)
[Back](#)
[Close](#)
[Print Version](#)
[Interactive Discussion](#)

© EGS 2001

In the aqueous phase the resident concentrations of both HO_{2(aq)} and NO_{2(aq)} decrease by ~ 4% and ~ 20%, respectively, comparing case (V) to case (III) (not shown) as a result of the changes in the resident concentrations for the associated species in the gas phase. The only appreciable consequence of this is a marginal increase in the concentrations of radical cations such as Br₂⁻. This is a result of a somewhat smaller efficiency of the terminating reactions involving HO_{2(aq)} and a small change in the speciation of Fe (< 2%). There are no effects due to NO_{2(aq)} which is too a large extent chemically inert once in solution (neglecting equilibrium (14)). One further difference which occurs in the absence of HNO_{4(aq)} is a small decrease in [O_{3(aq)}] and [H₂O_{2(aq)}] due to the oxidation of S(IV) by HNO_{4(aq)}, R25, being a significant pathway for sulphate production (Warneck, 1999).



In summary, the net aqueous phase conversion of NO₂ to NO seems to have little effect on the overall chemistry which occurs in solution since the reaction cycle R12–R13–R15–R16–R17 is relatively independent of other oxidants. This point is discussed in more detail below in the section concerned with uncertainties.

4.2. The effect of NO₃⁻ photolysis on HONO_(g) production

Case (VI) is presented to investigate whether the photolysis of NO₃⁻, R9, contributes significantly to the release of HONO_g as a result of the in situ production of NO_{2(aq)}. This is interesting in that R9 provides a means of re-activating NO₃⁻ into NO_x, i.e. it does not simply act as a sink for NO_x, which previous modelling studies have tended to ignore. Moreover, typical [NO₃⁻] obtained in our simulations are in the range of 2 × 10⁻⁵ mol dm⁻³ meaning that, although the rate of R9 is rather small (J_{max} = 4.3 × 10⁻⁷ s⁻¹), the production of NO_{2(aq)} could still be relatively efficient during summer at mid-latitudes. Consequently the efficiency of equilibrium (14) is not limited by K_H(NO₂). Once formed in situ, NO_{2(aq)} can either react with HO_{2(aq)} to form HNO_{4(aq)}, equilibrium (14), or escape back into the gas phase, with the branching ratio being pH dependent,

**Clouds, HO_x and NO_x
in the MBL**J. E. Williams et al.

[Title Page](#)[Abstract](#)[Introduction](#)[Conclusions](#)[References](#)[Tables](#)[Figures](#)[◀](#)[▶](#)[◀](#)[▶](#)[Back](#)[Close](#)[Print Version](#)[Interactive Discussion](#)

© EGS 2001

i.e. the speciation of HO_{2(aq)}. For brevity only differences in concentrations of > 2% between cases (III) (cloud only) and case (VI) will be discussed here. The most important effect of neglecting R9 is that the simulated increase in [HONO_g], due to the presence of cloud, decreases by ~ 5% (Fig. 5a), which, in turn, causes associated decreases in [OH_g], [NO_g] and [NO_{2(g)}]. This effect can be explained by considering the corresponding decrease in [HNO_{4(aq)}] and [HONO_(aq)] by ~ 5% (not shown) suggesting that R9 does make a slight contribution to the release of HONO_g. Another interesting feature is that the ratio for NO_{2(g)} between cases (III) (cloud only) and (VI) decreases by ~ 13% compared to Table 10a. This is most probably a cumulative effect of the direct release of NO₂ from the cloud and the differences introduced by the decrease in HONO_g, i.e. lower (OH_g).

4.3. The effect of halogen chemistry on HONO_(g) production

Case (VII) investigates whether aqueous phase halogen chemistry has any significant influence on the release of HONO_g, e.g by altering the acidity of the cloud droplets or by introducing a competing reaction pathway, which alters the efficiency in the formation of [HONO_(aq)]. The release of reactive halogen species from sea-salt aerosol in the polluted MBL has been the subject of a host of modeling studies (Sander and Crutzen, 1996; Vogt et al., 1996; Sander et al., 1999), which have concluded that such species have the potential to significantly deplete O_{3(g)} via an auto-catalytic chain reaction. Under the relatively unpolluted scenario chosen here, comparing the ratios between case (VII) (not shown) and case (III) reveals that, in the absence of deliquescent aerosol, the simulated change in [O₃]_g in a cloud only simulation is a result of a change in NO_x chemistry and not due to reactive halogen chemistry. This maybe explained by considering the mechanism by which the halogen species are released, which relies on the conversion of BrOH to BrCl (Vogt et al., 1996), equilibrium (26);



In dilute solution both $[H^+]$ and $[Cl^-]$ are much lower than that found in aerosol associated water therefore the effective formation rate of BrCl is also much lower, which seems to limit the importance of this equilibrium in cloud droplets. As a result the ratios obtained for cases (III) (cloud only) and (VII) (cloud only – no halogen chemistry) are very similar, i.e. differences in $[O_{3(g)}]$ and $[NO_{x(g)}]$ are $< 1\%$. Therefore, the majority of the detailed halogen chemistry listed in Table 5 seems only to be significant in our model when the aerosol chemistry is active (case IV).

5. Discussion

5.1. Other model studies

From the sensitivity studies presented in the preceding sections it can be seen that introducing the $HNO_{4(aq)}$ reaction sequence (R7–R12–R13–R15–R16–R17) into the aqueous phase chemistry substantially modifies the resident concentrations of many of the most important gas phase oxidants. To the authors knowledge, the only other modelling studies which have included such a mechanism in their cloud chemistry schemes are those of Liu et al. (1997), Warneck (1999) and Herrmann et al. (2000a). However, in these previous studies, the EURAD CTM column model of Liu et al. (1997) was concerned with a polluted continental scenario (i.e. high emissions and low cloud pH) whilst the box-modelling studies of Warneck (1999) and Herrmann et al. (2000a) focused more on heterogeneous sulphate production rather than the effects of cloud on gas phase NO_x . More recently, Dentener et al. (2001) included the uptake and heterogeneous reactions of $HNO_{4(g)}$ in a 3D global CTM, where substantial changes were simulated for $[O_{3(g)}]$ (-2 to 10%), $[SO_{2(g)}]$ (10 to 20%) and $[H_2O_{2(g)}]$ (-2 to 20%) in the boundary layer as a result. However, due to the computational limitations associated with such a study the heterogeneous uptake of HO_x species was ignored meaning that the formation of $HNO_{4(g)}$ and the consequent heterogeneous uptake of $HNO_{4(g)}$ may have been somewhat overestimated. Therefore, it is difficult to make quantitative

[Title Page](#)[Abstract](#)[Introduction](#)[Conclusions](#)[References](#)[Tables](#)[Figures](#)[I◀](#)[▶I](#)[◀](#)[▶](#)[Back](#)[Close](#)[Print Version](#)[Interactive Discussion](#)

© EGS 2001

comparisons of the results in our study and the aforementioned studies.

5.2. Effect on ozone

Table 12 summarises the variation in the NO/NO_x ratio for cases (I)–(VI), where the comparisons are segregated into the same height regimes as those used in Tables 10 and 11. Although, the differences in the NO/NO_x ratio between the cases presented here are quite small, it can be seen by comparing Figs. 6a and b that $[\text{NO}_g]$ increases by up to 5 nmol/mol as a result of heterogeneous conversion of NO_2 . This, in conjunction with the associated increase in $\text{NO}_{2(g)}$, Fig. 7a, results in the production of $\text{O}_{3(g)}$ for case (III) to be more efficient than case (V) as a result of R6 and R18. However, it must be noted that there is still a $\sim 2\%$ decrease in $\text{O}_{3(g)}$ by the fifth day, due to the large depletion of $[\text{HO}_{2(g)}]$. This implies that using an aqueous phase chemical mechanism, which neglects the heterogeneous HNO_4 reaction cycle discussed here, will result in an over-estimation of the effects of cloud on the tropospheric $\text{O}_{3(g)}$ budget. A further effect of the elevation of HONO_g is the regeneration of OH_g when clouds are present (compare Tables 10a and 11). Although the monthly averaged global cloud fraction is estimated to be only $\sim 30\%$ (ISCCP, 1995), this regeneration could still have important implications regarding the lifetime of greenhouse gases such as CO_g and $\text{CH}_{4(g)}$, which serve as the main sinks for OH_g . However, it is difficult to estimate the long-term global effect of this finding as CO_g emissions from anthropogenic sources will also have high levels of other pollutants which would limit the efficiency of the NO_2 conversion mechanism discussed here.

5.3. Uncertainties in reaction rates

The simulated conversion of NO_2 to NO due to the presence of cloud, as presented in this study, relies heavily on the validity of a number of assumptions made regarding the reactivity of nitrogen species in both the gas phase and in aqueous solution. The uncertainty in the equilibrium constant for $\text{HNO}_{4(g)}$ is listed as a factor of 5 (DeMore

Title Page

Abstract

Introduction

Conclusions

References

Tables

Figures

◀

▶

◀

▶

Back

Close

Print Version

Interactive Discussion

**Clouds, HO_x and NO_x
in the MBL**

 J. E. Williams et al.

[Title Page](#)
[Abstract](#)
[Introduction](#)
[Conclusions](#)
[References](#)
[Tables](#)
[Figures](#)
[I◀](#)
[▶I](#)
[◀](#)
[▶](#)
[Back](#)
[Close](#)
[Print Version](#)
[Interactive Discussion](#)

© EGS 2001

et al., 1997). Analysis of recent measurements, which were performed under clear sky conditions in the free troposphere have suggested that $[\text{HNO}_{4(\text{g})}]$ is lower than expected (Brune et al., 1999). If indeed the equilibrium constant for $\text{HNO}_{4(\text{g})}$ is lower than that described in RACM (as suggested by Brune et al., 1999) then the amount of HNO_4 transferred into solution would decrease according to the change in the partial pressure. Under these circumstances the heterogeneous conversion of HNO_4 could become rather trivial. In terms of the uncertainties concerning the reactivity of NO_x in solution, the reaction cycle R7–R12–R13–R15–R16–R17 does not depend on radicals or other species. However, this is, in part, due to insufficient knowledge and a scarcity of data available for processes which occur in the liquid phase. For instance, the most important free-radical oxidant in the atmospheric aqueous phase is considered to be the OH radical, where many of its reactions occur at, or near, the diffusion-controlled limit (i.e. $10^{10} \text{ M}^{-1} \text{ s}^{-1}$). Therefore, it seems most likely that interactions between OH and NO_x reservoir species could occur, such as reactions (27) to (29);



The consequence of such reactions would be to hinder the release of HONO_g by allowing a competing pathway for the indirect oxidation of NO to NO_2 whilst consuming two radicals. However, for these reactions to be significant the resident concentrations of these NO_x reservoir species must be of a similar magnitude as the other solutes which are thought to be efficient scavengers for OH_{aq} (e.g. HCOO^-), assuming similar rate constants. Comparing typical concentrations for case (III) reveals that this is not the case, with $[\text{HCOO}^-]/([\text{HNO}_2] + [\text{HONO}]) \approx 10^3$. Therefore, the influence of OH_{aq} on the conversion of NO_2 is probably small. One further omission is the oxidation of HONO_{aq} by H_2O_2 , R30. However, due the reaction rate for this process being relatively

slow ($k_{28} = 6.3 \times 10^3 \text{ M}^{-1} \text{ s}^{-1}$) and dependent on (H^+), the influence on $[\text{HONO}_{\text{aq}}]$ is considered to be negligible;



In terms of the existing data, the rate constant concerned with the aqueous phase NO_x chemistry, which has the most associated uncertainty is that for the unimolecular dissociation of NO_4^- , (R15). The value used here (0.8 s^{-1}) is taken from the modelling study of Warneck (1999) which is an average of the two available literature values of Lammel et al. (1990) and Logager and Sehested (1993). In their study Logager and Sehested (1993) suggest that the rate for this process could be up to 200 s^{-1} , which would increase the overall conversion rate of NO_2 significantly. Therefore, in view of this fact, this study could be a lower limit in terms of the production efficiency of HONO_{g} . Moreover, this highlights the need for further experimental studies concerning the behaviour of such species in solution.

In a recent study concerned with the photolytic production of OH_{aq} in fog waters during winter, Anastasio and McGregor (2001) claim that between 47–100% of photoformed OH_{aq} originates from the photolysis of $\text{NO}_2^-/\text{HONO}$, reaction (31), with the photolysis of nitrate, R9, being a relatively minor source;



However, using a photolysis rate calculated from the data of Zellner et al. (1990), this reaction was found to be relatively insignificant during the construction of CAPRAM 2.4 (Herrmann et al., 2000b). Nevertheless, if this reaction is more important than previously thought the most significant effect would be to reduce the regeneration of OH_{g} . The $\text{NO}_{(\text{aq})}$ formed would escape back into the gas phase due to its low solubility, so that any net decrease in the NO_{g} would result as an indirect effect of the fluctuation of OH_{g} .

Due to the fact that the chemical environments found in/on deliquescent aerosol and in cloud droplets are quite different (e.g. pH, ionic strength) one of the largest assumptions made here is that a generic reaction mechanism can adequately account

**Clouds, HO_x and NO_x
in the MBL**J. E. Williams et al.

Title Page

Abstract

Introduction

Conclusions

References

Tables

Figures

I◀

▶I

◀

▶

Back

Close

Print Version

Interactive Discussion

**Clouds, HO_x and NO_x
in the MBL**J. E. Williams et al.

[Title Page](#)[Abstract](#)[Introduction](#)[Conclusions](#)[References](#)[Tables](#)[Figures](#)[I◀](#)[▶I](#)[◀](#)[▶](#)[Back](#)[Close](#)[Print Version](#)[Interactive Discussion](#)

© EGS 2001

for the chemistry, which occurs in both phases. The results presented for case (VII) suggest that certain processes, which have been found to be important on deliquescent aerosol become less important in cloud droplets, and the opposite will also be true. The CAPRAM 2.4. mechanism was condensed using a standard cloud box-model (Herrmann et al., 2000b) therefore certain reactions may have been omitted from the mechanism which could have important effects when trying to simulate gas-aerosol chemistry. This is the reason why we supplemented the aqueous phase reaction scheme with the extra reaction set given in Table 5. Moreover, generic K_H and α values for both phases have been implemented which may also be an over simplification. For example, laboratory investigations have recently found that the $K_H(\text{HONO})$ may differ by an order of magnitude depending on the concentration of ammonium sulphate solutions (Becker et al., 1998) which would have implications regarding the uptake by deliquescent aerosol. Unfortunately, to the authors knowledge, no corresponding measurements have been made for other important HO_x and NO_x species.

5.4. Other uncertainties

The results presented in this paper focus on the effects of aqueous phase HNO₄ chemistry during daytime but it is also pertinent to discuss the effect during nighttime. In the absence of photolysing light, the resident [HO_{2(g)}] falls substantially (Fig. 3b) causing a corresponding decrease in [HNO_{4(g)}] via R12 (not shown). However, the release of HONO_g still occurs over the first few hours of a night as shown in Fig. 5a. This infers that there is sufficient HNO₄/NO₄⁻ retained in solution to ensure the production of NO₂⁻, via R13, even when the [HNO_{4(g)}] decreases. During wintertime at mid-latitudes the production rate of HNO_{4(g)} will be reduced due to the lower concentration of HO_{2(g)} (less intense sunlight) and long nights. On the other hand the lower temperatures would prolong the gas phase lifetime of HNO₄. Indeed the results of Dentener et al. (2001) suggested a rather constant effect on photo-oxidants throughout the seasons, with somewhat larger effects during the SH summer and NH winter. As indicated before computational limitations meant that we did not attempt to simulate such a range of

locations and seasons in this study.

Although the chemical reaction mechanism discussed here could produce a significant amount of HONO_g in unpolluted locations it is likely to become relatively inefficient in more polluted scenarios. This is principally due to the high anthropogenic emissions which are associated with such areas which usually result in typical pH values for atmospheric aerosol droplets to be much lower than in our simulations ($\sim\text{pH } 3\text{--}4$) which alters the ratio of $\text{HNO}_4 : \text{NO}_4^-$. Therefore, even though there will be the higher level of NO_x present in such scenarios, which will result in a subsequent elevation in $[\text{HNO}_{4(g)}]$, the uptake will be dictated by $K_H(\text{HNO}_4)$ and R25 rather than equilibrium (13). Moreover, the soluble organic fraction will be much more diverse in a polluted scenario compared to that found in the MBL, which introduces uncertainties as to whether the NO_x reservoir species would not be oxidised by other processes in such an environment. Furthermore, the only CCN considered in our model are ammonium sulphate and sea-salt particles, which originate from the sea surface. However, in more polluted air masses continental dust particles would also contribute significantly to the CCN, which could introduce inhomogeneity between cloud droplets. In view of these points, we suggest that the reduction of $\text{HNO}_{4(g)}$ in cloud will simply be one of a number of heterogeneous pathways which could contribute to the production of HONO_g over the continent, e.g. conversion on anthropogenic aerosol.

Finally, we acknowledge that the 1-D model used here focuses on the effects introduced by a non-precipitating marine stratocumulus cloud whereas, under certain meteorological conditions, both drizzle and rain maybe important sinks for the fraction of NO_x reservoir species which are dissolved. For example, in the aforementioned study by Anastasio and McGregor (2001) measured $[\text{N}^{\text{III}}] \approx \mu\text{M}$ levels from size-segregated cloud water samples near Tenerife. Thus, loss of NO_2^- via precipitation would mean that the regeneration of HO_x and NO_x from the cloud would be less efficient than that simulated here, which would have consequences for both the lifetime of trace gases in the MBL and the production of $\text{O}_{3(g)}$. However, our study is more representative of most dominant non-precipitating clouds.

Clouds, HO_x and NO_x
in the MBL

J. E. Williams et al.

Title Page

Abstract

Introduction

Conclusions

References

Tables

Figures

◀

▶

◀

▶

Back

Close

Print Version

Interactive Discussion

© EGS 2001

6. Conclusions

In this study we have included a comprehensive aqueous phase chemical mechanism into a 1-D stratocumulus cloud model for the purpose of simulating the heterogeneous effects of cloud on gas phase concentrations of HO_x and NO_x . We have found that, during summertime at mid-latitudes (45°N), the heterogeneous reduction of $\text{HNO}_{4(\text{g})}$ by cloud can act as a source of HONO_g in the unpolluted MBL. The reaction sequence which leads to this is critically dependent on the pH of the cloud-water. Therefore, it is most likely to be important only in remote locations away from strong anthropogenic emissions. Furthermore, we have shown that the photolysis of NO_3^- in solution contributes by $\sim 5\%$ to this simulated increase in HONO_g and therefore may also be a minor source of $\text{NO}_{2(\text{g})}$. As a result of both reaction sequences, both OH_g and NO_x concentrations are found to increase compared to a simulation that neglects the aqueous phase chemistry of $\text{HNO}_{4(\text{aq})}$ and the photolysis of NO_3^- . This elevation in NO_x results in a reduction in the simulated perturbation of $\text{O}_{3(\text{g})}$ due to cloud, i.e. it causes the system to move more towards the 'compensation' point for $\text{O}_{3(\text{g})}$. It has been speculated previously that clouds, in addition to their radiative effects, exert a strong influence on OH_g . However, as we have shown in this paper, the regeneration of OH_g provides a strong feedback mechanism and reduces the influence of clouds on the overall oxidising capacity of the marine boundary layer and the lifetime of important greenhouse gases such as $\text{CH}_{4(\text{g})}$. The effect of introducing deliquescent aerosol into the simulations is rather insignificant due to the limited uptake of $\text{HNO}_{4(\text{g})}$ in the aerosol associated water. We therefore suggest that future modelling studies concerned with the heterogeneous effects of cloud on gas phase oxidants include the $\text{HNO}_{4(\text{g})}$ reaction sequence as presented here. However, considering the large uncertainties involved with the aqueous phase chemistry, mechanism, the computational limitations of including such chemistry, and the moderate effects on photo-chemistry of including the aqueous phase mechanism relative to other uncertainties currently associated with 3D global CTMs, we do not feel that the aqueous phase chemistry of $\text{HNO}_{4(\text{g})}$ should be imple-

Clouds, HO_x and NO_x in the MBL

J. E. Williams et al.

Title Page

Abstract

Introduction

Conclusions

References

Tables

Figures

◀

▶

◀

▶

Back

Close

Print Version

Interactive Discussion

© EGS 2001

mented until a more sophisticated and less uncertain understanding of heterogeneous uptake becomes available. Furthermore, we suggest that more laboratory work should be conducted concerning the rate of uptake of HO_x and NO_x species by concentrated salt solution.

5 *Acknowledgements.* J. E. W. gratefully acknowledges financial support from the COACH funding program and the Foundation for Fundamental Research on Matter (FOM).

References

Anastasio, C. and McGregor, K. G., Chemistry of fog waters in California's Central Valley: 1. In situ photoformation of hydroxyl radical and singlet molecular oxygen, *Atmos. Environ.*, 35, 1079–1089, 2001.

10

Aranda, A., Le Bras, G., La Verdet, G., and Poulet, G., The BrO + CH₃O₂ reaction: Kinetics and role in the atmospheric ozone budget, *Geophys. Res. Letts.*, 24, 2745–2748, 1997.

Atkinson, R., Baulch, D. L., Cox, R. A., Hampson, R. F., and Troe, J., Evaluated kinetic and photochemical data for atmospheric chemistry: Supplement IV, *J. Phys. Chem. Ref Data*, 21, 1125–1444, 1992.

15

Baboukas, B. D., Kanakidou, M., and Milhalopolous, N., Carboxylic acids in gas and particulate phase above the Atlantic Ocean, *J. Geophys. Res.*, 105, 14459–14471, 2000.

Barnes, I, Bastain, V., and Becker, K. H., Oxidation of organic sulphur compounds, In: *The Tropospheric Chemistry of Ozone in the Polar Regions*, NATO ASI Series 17, Niki, H. and Becker, K. H., (Eds) 371–383, Springer-Verlag, Berlin, 1993.

20

Bambauer, A., Brantner, B., Paige, M., and Novakov, T., Laboratory study of NO₂ reaction with dispersed and bulk liquid water, *Atmos. Environ*, 20, 3225–3332, 1994.

Becker, K. H., Kleffmann, J., Negri, R. M., and Wiesen, P., Solubility of nitrous acid (HONO) in ammonium sulphate solutions, *J. Chem. Soc. Faraday. Trans.*, 94, 1583–1586, 1998.

25

Behnke, W., George, C., Scheer, V., and Zetzsch, C., Production and decay of ClNO₂ from the reaction of gaseous N₂O₅ with NaCl solution: Bulk and aerosol experiments, *J. Geophys. Res.*, 102, 3795–3804, 1997.

Brune, W. H., et al., OH and HO₂ chemistry in the North Atlantic free troposphere, *Geophys. Res. Letters*, 26, 3077–3080, 1999.

Clouds, HO_x and NO_x in the MBL

J. E. Williams et al.

Title Page

Abstract

Introduction

Conclusions

References

Tables

Figures

◀

▶

◀

▶

Back

Close

Print Version

Interactive Discussion

**Clouds, HO_x and NO_x
in the MBL**J. E. Williams et al.

[Title Page](#)[Abstract](#)[Introduction](#)[Conclusions](#)[References](#)[Tables](#)[Figures](#)[I◀](#)[▶I](#)[◀](#)[▶](#)[Back](#)[Close](#)[Print Version](#)[Interactive Discussion](#)

© EGS 2001

- Calvert, J. G., Yarwood, G., and Dunker, A. M., An evaluation of the mechanism of nitrous acid formation in the urban atmosphere, *Research on Chem. Inter.*, 20, 463–502, 1994.
- Chameides, W. L. and Davis, D. D., The free radical chemistry of cloud droplets and its impact upon the composition of rain, *J. Geophys. Res.*, 87, 4863–4877, 1982.
- 5 Cooke, W. F., Jennings, S. G., and Spain, T. G., Black carbon measurements at Mace Head 1989–1996, *J. Geophys. Res.*, 102, 25 339–25 346, 1997.
- Crutzen, P. J., Ozone in the troposphere, in *Composition, Chemistry and climate of the Atmosphere*, edited by Singh, H. B., pp 349–393, Van Nostrand Reinhold, New York, 1995.
- Davies, J. A. and Cox, R. A., Kinetics of the heterogeneous reaction of HNO₃ with NaCl: Effect
10 of water vapour, *J. Phys. Chem.*, 102, 7631–7642, 1998.
- Dentener, F. J. and Crutzen, P. J., Reaction of N₂O₅ on tropospheric aerosols: impact on the global distributions of NO_x, O₃ and OH, *J. Geophys. Res.*, 98, 7149–7162, 1993.
- Dentener, F. J., Williams, J. E., and Metzger, S. M., The Aqueous Phase reaction of HNO₄: the impact on tropospheric chemistry, *J. Atmos. Chem.*, accepted for publication, 2001.
- 15 DeMore, W. B., Sander, S. P., Golden, D. M., Hampson, R. F., Kurylo, M. J., Howard, C. J., Ravishankara, A. R., Kolb, C. E., and Molina, M. J., Chemical kinetics and Photochemical data for use in stratospheric modeling, JPL publication 92–94, Jet Propulsion Laboratory, Pasadena, CA, 1997.
- Duynkerke, P. G. and Driedonks, A. G. M., A model for the turbulent structure of the
20 Stratocumulus-topped atmospheric boundary layer, *J. Atmos. Sci.*, 44, 43–64, 1987.
- Fenter, F. F., Caloz, F., and Rossi, M. J., Heterogeneous kinetics of N₂O₅ uptake on salt, with a systematic study of the role of surface presentation (for N₂O₅ and HNO₃), *J. Phys. Chem.*, 100, 1008–1019, 1996.
- Fitzgerald, J. W., Approximation formulas for the equilibrium size of an aerosol particle as a
25 function of its dry size and composition and the ambient relative humidity, *J. Appl. Meteorol.*, 14, 1044–1049, 1975.
- Flossmann, A. I., Hall, W. D., and Pruppacher, H. R., A theoretical study of the wet removal of atmospheric pollutants, In: *The redistribution of aerosol particles captured through nucleation and impactation scavenging by growing cloud droplets*, *J. Atmos. Sci.*, 42, 583–606, 1985.
- 30 Fortnum, K. D., Battaglia, C. J., Cohen, S. R., and Edwards, J. O., The kinetics of the oxidation of halide ions by monosubstituted peroxides, *J. Am. Chem. Soc.*, 82, 778–782, 1960.
- Fogelman, K. D., Walker, D. M., and Margerum, D. W., Non-metal redox kinetics: Hypochlorite

- and hypochlorous acid reactions with sulfite, *Inorg. Chem.*, 28, 986–993, 1989.
- Gerecke, A., Theilman, A., Gutzwiller, A., and Rossi, M. J., The chemical kinetics of HONO formation resulting from heterogeneous interaction of NO₂ with flame soot, *Geophys. Res. Lett.*, 25, 2453–2456, 1998.
- 5 Greadel, T. E. and Weschler, C. J., Chemistry within aqueous atmospheric aerosols and raindrops, *Rev. Geophys. Space. Phys.*, 19, 505–539, 1981.
- Grenfell, J. L., et al., Tropospheric box-modelling and analytical studies of the hydroxyl (OH) radical and related species: Comparison with observations, *J. Atmos. Chem.*, 33, 183–214, 1999.
- 10 Haag, W. R. and Hoigne, J., Ozonation of bromine-containing waters: Kinetics of formation of hypobromous acid and bromate, *Environ. Sci. Tech.*, 17, 261–267, 1983.
- Harrison, R. M., Peak, J. D., and Collins, G.M., Tropospheric cycle of nitrous acid, *J. Geophys. Res.*, 101, 14 429–14 439, 1996.
- Harrison, R. M. and Collins, G. M., Measurements of reaction coefficients of NO₂ and HONO on aerosol particles, *J. Atmos. Chem.*, 30, 397–406, 1998.
- 15 Heikes, B. G., Lee, M., Jacob, D. J., Talbot, R. W., Bradshaw, J. D., Singh, H. B., Blake, D. R., Anderson, B. E., Fuelberg, H. E., and Thompson, A. M., Ozone, hydroperoxides, oxides of nitrogen, and hydrocarbon budgets in the marine boundary layer over the South Atlantic, *J. Geophys. Res.*, 101, 24 221–24 234, 1996.
- 20 Herrmann, H., Ervens, B., Jacobi, H.-W., Wolke, R., Nowacki, P., and Zellner, R., CAPRAM 2.3: A chemical aqueous phase radical mechanism for tropospheric Chemistry, *J. Atmos. Chem.*, 36, 231–284, 2000(a).
- Herrmann, H., Buxton, G. V., Salmon, G. A., Mirabel, P., George, C., Lelieveld, J., and Dentener, F., Model Development for Tropospheric Aerosol and Cloud Chemistry (MODAC), final report, EU contract No. ENV4-CT97-0388, 2000(b).
- 25 Houghton, J. T., Filho, M., Callander, B. A., Harris, N., Katzenberg, A., and Maskell, K., eds., Intergovernmental Panel on Climate Change (IPCC), *Climate Change 1995, The science of climate change*, Cambridge University Press, Cambridge, U. K., 1995.
- Jacob, D. J., The chemistry of OH in remote clouds and its role in the production of formic acid and peroxymonosulphate, *J. Geophys. Res.*, 91, 9807–9826, 1986.
- 30 Jacob, D. J., Heterogeneous chemistry and tropospheric ozone, *Atmos. Environ.*, 34, 2131–2159, 2000.
- Jaegle, W., et al., Photochemistry of HO_x in the upper troposphere at northern mid-latitudes, *J.*

**Clouds, HO_x and NO_x
in the MBL**J. E. Williams et al.

[Title Page](#)[Abstract](#)[Introduction](#)[Conclusions](#)[References](#)[Tables](#)[Figures](#)[◀](#)[▶](#)[◀](#)[▶](#)[Back](#)[Close](#)[Print Version](#)[Interactive Discussion](#)

© EGS 2001

**Clouds, HO_x and NO_x
in the MBL**J. E. Williams et al.

[Title Page](#)[Abstract](#)[Introduction](#)[Conclusions](#)[References](#)[Tables](#)[Figures](#)[I◀](#)[▶I](#)[◀](#)[▶](#)[Back](#)[Close](#)[Print Version](#)[Interactive Discussion](#)

© EGS 2001

Geophys. Res., 105, 3877–3892, 2000.

Jefferson, A., Nicovich, J. M., and Wine, P. H., Temperature-dependent kinetics studies of the reactions $\text{Br}(^2\text{P}_{3/2}) + \text{CH}_3\text{SCH}_3 \rightleftharpoons \text{HBr} + \text{CH}_3\text{SCH}_2$ Heat of formation of the CH_3SCH_2 radical, J. Phys. Chem., 98, 7128–7135, 1994.

5 Kalberer, M., Ammann, M., Arens, F., Gaggeler, H. W., and Baltensperger, U., Heterogeneous formation of nitrous acid (HONO) on soot aerosol particles, J. Geophys. Res., 104, 13 825–13 832, 1999.

Kelley, C. M. and Tartar, H. V., On the system: bromine-water, J. Am. Chem. Soc. 78, 5752–5756, 1959.

10 Kleffmann, J., Becker, K. H., Lackoff, M., and Wiesen, P., Heterogeneous conversion of NO_2 on Carbonaceous surfaces, Phys. Chem. Chem. Phys., 24, 5443–5450, 1999.

Krischke, U., Staubes, R., Brauers, T., Gautrois, M., Burkert, J., Stobener, D., and Jaeschke, W., Removal of SO_2 from the marine boundary layer over the Atlantic Ocean: a case study on the kinetics of the heterogeneous S(IV) oxidation on marine aerosols, J. Geophys. Res., 15 105, 14 413–14 422, 2000.

Krol, M. C. and van Weele, M., Implications of variations in photodissociation rates for global tropospheric chemistry, Atmos. Environ., 31, 1257–1273, 1997.

Kumer, K. and Margerum, D. W., Kinetics and mechanism of general-acid-assisted oxidation of bromide by hypochlorite and hypochlorous acid, Inorg. Chem., 26, 2706–2711, 1987.

20 Lammel, G., Perner, D., and Warneck, P., Decomposition of Pernitric Acid in Aqueous solution, J. Phys. Chem., 6141–6144, 1990.

Landgraf, J. and Crutzen, P. J., An efficient method for ‘On-Line’ calculations of photolysis and heating rates, J. Atmos. Sci., 55, 863–878, 1998.

Lawrence, M. G. and Crutzen, P. J., The impact of cloud particle gravitational settling on soluble trace gas distributions, Tellus 50B, 263–289, 1998.

25 Lax, E., Taschenbuch für Chemiker und Physiker, Springer Verlag, Berlin, 1969.

Lelieveld, J. and Crutzen, P. J., The role of clouds in tropospheric photochemistry, J. Atmos. Chem., 12, 229–267, 1991.

Liang, J. and Jacob, D. J., Effect of aqueous phase cloud chemistry on tropospheric ozone, J. Geophys. Res., 102, 5993–6001, 1997.

30 Liang, J. and Jacobson, M. Z., A study of sulfur dioxide oxidation pathways over a range of liquid water contents, pH values and temperatures, J. Geophys. Res., 10, 13 749–13 769, 1999.

**Clouds, HO_x and NO_x
in the MBL**J. E. Williams et al.

Title Page

Abstract

Introduction

Conclusions

References

Tables

Figures

I◀

▶I

◀

▶

Back

Close

Print Version

Interactive Discussion

© EGS 2001

Liu, X., Mauersberger, G., and Moller, D., The effects of cloud processes on the tropospheric photochemistry: an improvement of the EURAD model with a coupled gaseous and aqueous phase chemical mechanism, *Atmos. Environ.*, 31, 3119–3135, 1997.

Logager, T. and Sehested, K., Formation and Decay of Peroxynitric Acid: a Pulse radiolysis study, *J. Phys. Chem.*, 97, 10 047–10 052, 1993.

Longfellow, C. A., Ravishankara, A. R., and Hanson, D. R., Reactive uptake of hydrocarbon soot: focus on NO₂, *J. Geophys. Res.*, 104, 13 833–13 840, 1999.

Mallard, W. G., Westley, F., Herron, J. T., Hampson, R. F., and Frizzel, D. H., NIST chemical kinetics database: version 5.0, Gaithersburg, MD.

Matthijssen, J., Builtjes, P. J. H., and Sedlak, D. L., Cloud model experiments of the effect of iron and copper on tropospheric ozone under marine and continental conditions under marine and continental conditions, *Meteo. Atmos. Phys.*, 57, 43–60, 1995.

McFadyan, G. G. and Cape, J. N., Spring time sources and sinks of Peroxyacetyl Nitrate in the UK and its contribution to acidification and nitrification of cloud water, *Atmos. Res.*, 50, 359–371, 1999.

Moller, D. and Mauersberger, G., An aqueous phase reaction mechanism, In: *Clouds: Models and Mechanisms (EUROTRAC Special Publications)*, 77–93, ISS Garmisch-Partenkirchen, Germany.

Monahan, E. C., Speil, D. E., and Davidson, K. L., A model of marine aerosol generation via whitecaps and wave distribution, in *Oceanic Whitecaps*, eds; Monahan, E. C. and MacNiocaill, G., pp 167–174, D. Reigel, Norwell, Mass., 1986.

O'Dowd, C. D. and Smith, M. H., Physico-chemical properties of aerosol over the North East Atlantic; Evidence for wind speed related sub-micron sea-salt aerosol production, *J. Geophys. Res.*, 98, 1137–1149, 1993.

O'Dowd, C. D., Lowe, J. A., Clegg, N., Smith, M. M., and Clegg, S. L., Modeling heterogeneous sulphate production in maritime stratiform clouds, *J. Geophys. Res.*, 105, 7143–7160, 2000.

Plass-Dulmer, C., Koppmann, R., Ratte, M., and Rudolph, J., Light nonmethane hydrocarbons in seawater, *Global Bio. Cycles*, 9, 79–100, 1995.

Ravishankara, A. R. and Longfellow, C. A., Reactions on tropospheric condensed matter, *Phys. Chem. Chem. Phys.*, 1, 5433–5441, 1999.

Roger, R. R. and Yau, M. K., *A short course in Cloud Physics*, 3rd edition, pp. 193, Pergamon, Tarrytown, N. Y., 1994.

Sander, R. and Crutzen, P. J., Model study indicating halogen activation and ozone destruction

**Clouds, HO_x and NO_x
in the MBL**J. E. Williams et al.

[Title Page](#)[Abstract](#)[Introduction](#)[Conclusions](#)[References](#)[Tables](#)[Figures](#)[I◀](#)[▶I](#)[◀](#)[▶](#)[Back](#)[Close](#)[Print Version](#)[Interactive Discussion](#)

© EGS 2001

in polluted air masses transported to the sea., *J. Geophys. Res.*, 101, 9121–9138, 1996.

Sander, R., Rudich, Y., von Glasow, R., and Crutzen, P. J., The role of BrNO₃ in marine tropospheric chemistry: a model study, *Geophys. Res. Lett.*, 26(18), 2857–2860, 1999.

Sander, R. and von Glasow, R., personal communication, 2000.

5 Saxena, P. and Hildemann, L. M., Water-soluble organics in atmospheric particles: a critical review of the literature and application of thermodynamics to identify candidate compounds, *J. Atmos. Chem.*, 24, 57–109, 1996.

Schwartz, S. E., Mass transport considerations pertinent to aqueous phase reactions of gases in liquid water clouds, in *Chemistry of Multiphase Atmospheric Systems*, (Ed) Jaeschke, W.,
10 NATO ASI series, 6, 415–471, Springer, Berlin.

Schwartz, S. E. and White, W. H., Kinetics of the reactive dissolution of nitrogen oxides into aqueous solution, *Adv. Environ. Sci. Technol.*, 12, 1–115, 1983.

Schweitzer, F., Mirabel, P., and George, C., Multiphase chemistry of N₂O₅, ClNO₂ and BrNO₂,
15 *J. Phys. Chem.*, 102, 3942–3952, 1998.

Sempere, R. and Kawamura, K., Comparative distributions of dicarboxylic acids and related polar compounds in snow, rain and aerosols from urban atmosphere, *Atmos. Environ.*, 449–459, 1994.

Stickell, R. E., Nicovich, J. M., Wang, W., Zhao, Z., and Wine, P. H., Kinetic and mechanistic study of the reaction of atomic chlorine with dimethyl sulphide, *J. Phys. Chem.*, 58, 9875–9883, 1992.

20 Stockwell, W. R., Kirchner, F., Kuhn, M., and Seefeld, S., A new regional mechanism for regional atmospheric chemistry modeling, *J. Geophys. Res.*, 102, 25 847–25 879, 1997.

Troy, R. C. and Margerum, D. W., Non-metal redox kinetics: Hypobromite and hypobromous acid reactions with iodide and with sulfite and the hydrolysis of bromosulphate, *Inorg. Chem.*,
25 30, 3538–3543, 1991.

Van den Berg, A. R., Dentener, F. J., and Lelieveld, J., Modelling the chemistry of the Marine Boundary Layer; sulphate formation and the role of sea salt aerosol particles, *J. Geophys. Res.*, 105, 11 671–11 698, 2000.

Vogt, R., Crutzen, P. J., and Sander, R., A mechanism for halogen release from sea-salt aerosol in the remote marine boundary layer, *Nature*, 383, 327–330, 1996.

30 Wagner, I. and Strehlow, H., On the flash photolysis of bromide ions in aqueous solution, *Ber. Bunsenges. Phys. Chem.*, 91, 1317–1321, 1987.

Walcek, C. J., Yuan, H.-H., and Stockwell, W. R., The influence of aqueous-phase chemical

reactions on ozone formation in polluted and nonpolluted cloud, *Atmos. Environ.*, 31, 1221–1237, 1997.

Wang, T. X., Kelley, M. D., Cooper, J. N., Beckwith, R. C., and Margerum, D. W., Equilibrium, kinetic and UV-spectral characteristics of aqueous bromine chloride, and chlorine species, *Inorg. Chem.*, 33, 5872–5878.

Warneck, P., The relative importance of various pathways for the oxidation of sulfur dioxide and nitrogen dioxide in sunlit continental fair weather clouds, *Phys. Chem. Chem. Phys.*, 1, 5471–5483, 1999.

Zellner, R., Exner, M., and Herrmann, H., Absolute OH quantum yields in the laser photolysis of Nitrate, Nitrite and dissolved H_2O_2 at 308 and 351 nm in the temperature range 278–353 K, *J. Atmos. Chem.*, 10, 411–425, 1990.

Zhang, Y., Bischof, C. H., Easter, R. C., and Wu, P.-T., Sensitivity analysis of a mixed-phase chemical mechanism using automatic differentiation, *J. Geophys. Res.*, 103, 18 953–18 979, 1988.

Zimmerman, J. and Poppe, D., A supplement for the RADM2 chemical mechanism: The photooxidation of Isoprene, *Atmos. Environ.*, 30, 1255–1269, 1996.

**Clouds, HO_x and NO_x
in the MBL**

J. E. Williams et al.

Title Page

Abstract

Introduction

Conclusions

References

Tables

Figures

◀

▶

◀

▶

Back

Close

Print Version

Interactive Discussion

© EGS 2001

Table 1. List of chemical species considered in the 1-D model. For definitions of the abbreviations concerning the lumped species the reader is referred to Stockwell et al., 1997

Phase	Group	Species
Gas	S	SO ₂ , CH ₃ SCH ₃ , H ₂ SO ₄
	O	H ₂ O, H ₂ O ₂ , O(1) ^d , O(3) ^p , O ₂ , O ₃ , OH, HO ₂
	N	NH ₃ , HNO ₃ , NO, NO ₂ , NO ₃ , N ₂ O ₅ , HNO ₄ , PAN, TPAN
	C ^[a]	CO, CH ₄ , CO ₂ , CH ₂ O, CH ₃ OOH, HCO ₂ H, CH ₃ OH, CH ₃ O ₂ , C ₂ H ₄ , C ₂ H ₆ , C ₂ H ₅ OH, H ₂ C ₂ O ₄ , ETHP, ACO ₃ , PAA, ALD, KET, ORA2, OP2, GLY, MGLY, HC3, ISO, OLT, OLI, OLT, DIEN, HC5, ONIT, DCB, API, LIM, UDD, HKET, HC8, TOL, XYL, CSL, TCO3
	Cl	Cl, HCl, Cl ₂ , ClO, ClOH, ClNO ₂ , ClNO ₃ , Cl ₂ O ₂
	Br	Br, HBr, Br ₂ , BrO, BrOH, BrNO ₂ , BrNO ₃ , BrCl
H	H ₂	
Aqueous	S	SO ₂ , HSO ₃ ⁻ , SO ₃ ²⁻ , HSO ₄ ⁻ , SO ₄ ²⁻ , HSO ₅ ⁻ , HOCH ₂ SO ₃ ⁻ , SO ₄ ⁻ , SO ₅ ⁻ , CHOSO ₃ ⁻ , CHOHSO ₃ ⁻ , CHOSO ₃ ²⁻ , SO ₅ O ₂ H ⁻ , SO ₅ O ₂ ²⁻ , O ₂ CHOHSO ₃ ⁻
	O	H ₂ O, H ₂ O ₂ , O ₂ , O ₃ , OH, HO ₂ , O ₂ ⁻ , HO ₃ , O ₃ ⁻
	N	NH ₃ , NH ₄ ⁺ , HNO ₂ , NO ₂ , NO ₂ ⁻ , HNO ₃ , NO ₃ ⁻ , HNO ₄ , NO ₄ ⁻ , N ₂ O ₅ , NO ₂ ⁺ , NO ₃
	C	CO ₂ , HCO ₃ ⁻ , CH ₂ O, CH(OH) ₂ , CH ₃ OOH, CH ₃ O ₂ , H ₂ C ₂ O ₄ , HC ₂ O ₄ ⁻ , C ₂ O ₄ ²⁻ , HCO ₂ H, HCO ₂ ⁻ , CH ₃ OH, CH ₃ CHO, CH ₃ CH(OH) ₂ , CH ₃ COOH, CH ₃ CO ₂ ⁻ , CH ₃ CH ₂ OH, CHOCHO, CH(OH) ₂ CH(OH) ₂ , CH(OH) ₂ COOH, CH(OH) ₂ COO ⁻ , ETHP, ACO ₃ , O ₂ CHO, CH ₃ CO, CH ₃ C(OH) ₂ , O ₂ CH ₂ OH, O ₂ CH ₃ CHOH, O ₂ C(OH) ₂ CH(OH) ₂ , O ₂ C(OH) ₂ COOH, O ₂ C(OH) ₂ COO ⁻
	Cl	Cl, Cl ⁻ , Cl ₂ ⁻ , HCl, Cl ₂ , ClOH ⁻ , ClOH, ClO ⁻ , ClNO ₂
	Br	Br, Br ⁻ , Br ₂ ⁻ , HBr, Br ₂ , BrOH ⁻ , BrOH, BrO ⁻ , BrNO ₂ , BrCl, Br ₂ Cl ⁻ , BrCl ⁻
	TMI ^[b]	Cu ⁺ , Cu ²⁺ , Fe ²⁺ , Fe ³⁺ , Fe(OH) ²⁺ , FeO ²⁺ , FeC ₂ O ₄ ⁺ , Fe(C ₂ O ₄) ₂ ⁻

Clouds, HO_x and NO_x in the MBL

J. E. Williams et al.

Title Page

Abstract

Introduction

Conclusions

References

Tables

Figures

◀

▶

◀

▶

Back

Close

Print Version

Interactive Discussion

© EGS 2001

**Clouds, HO_x and NO_x
in the MBL**

 J. E. Williams et al.

[Title Page](#)
[Abstract](#)
[Introduction](#)
[Conclusions](#)
[References](#)
[Tables](#)
[Figures](#)
[I◀](#)
[▶I](#)
[◀](#)
[▶](#)
[Back](#)
[Close](#)
[Print Version](#)
[Interactive Discussion](#)

© EGS 2001

Table 1. Continued...

Phase	Group	Species
solid ^[c]	S	H ₂ SO ₄ , NH ₄ HSO ₄ , (NH ₄) ₂ SO ₄ , NaHSO ₄ , Na ₂ SO ₄ , FeSO ₄ , Fe ₂ (SO ₄) ₃ , CuSO ₄ , Cu ₂ (SO ₄)
	N	NaNO ₃ , NH ₄ NO ₃ , Fe(NO ₃) ₂ , Fe(NO ₃) ₃ , CuNO ₃ , Cu(NO ₃) ₂
	C	NaHCO ₃ , NH ₄ HCO ₃ , Fe(HCO ₃) ₂ , Fe(HCO ₃) ₃ , CuHCO ₃ , Cu(HCO ₃) ₂
	Cl	NaCl, NH ₄ Cl, FeCl ₂ , FeCl ₃ , CuCl, CuCl ₂
	Br	NaBr, NH ₄ Br

[a] For the intermediates formed in the gas-phase which do not participate in heterogeneous reactions are omitted. [b] Transition Metal Ions. [c] Species fixed into aerosol upon evaporation of a cloud droplet.

**Clouds, HO_x and NO_x
in the MBL**

 J. E. Williams et al.

Table 2. Gas phase photolysis rates used in the 1-D model

Number	Reaction	Note	Reference
J(1)	$\text{NO}_2 (+ \text{O}_2) + h\nu \rightarrow \text{NO} + \text{O}_3$	a	KW97
J(2)	$\text{O}_3 h\nu \rightarrow \text{O}^1(\text{d}) + \text{O}_2$	a	KW97
J(3)	$\text{O}_3 + h\nu \rightarrow \text{O}^3(\text{p}) + \text{O}_2$	a	Scaled to J(7)
J(4)	$\text{HONO} + h\nu \rightarrow \text{OH} + \text{NO}$	a	Scaled to J(1)
J(5)	$\text{HNO}_3 + h\nu \rightarrow \text{NO}_2 + \text{OH}$	a	KW97
J(6)	$\text{HNO}_4 + h\nu \rightarrow 0.65\text{HO}_2 + 0.65\text{NO}_2 + 0.35\text{OH} + 0.35\text{NO}_3$	a	KW97
J(7)	$\text{NO}_3 + h\nu \rightarrow \text{NO} + \text{O}_2$	a	KW97
J(8)	$\text{NO}_3 (+ \text{O}_2) + h\nu \rightarrow \text{NO}_2 + \text{O}_3$	a	KW97
J(9)	$\text{H}_2\text{O}_2 + h\nu \rightarrow \text{OH} + \text{OH}$	a	KW97
J(10)	$\text{HCHO} + h\nu \rightarrow \text{H}_2 + \text{CO}$	a	KW97
J(11)	$\text{HCHO} (+ \text{O}_2) + h\nu \rightarrow \text{HO}_2 + \text{HO}_2 + \text{CO}$	a	KW97
J(12)	$\text{ALD} + h\nu \rightarrow \text{CH}_3\text{O}_2 + \text{HO}_2 + \text{OH}$	a	KW97
J(13)	$\text{CH}_3\text{OOH} + h\nu \rightarrow \text{HCHO} + \text{HO}_2 + \text{OH}$	a	KW97
J(14)	$\text{OP2} + h\nu \rightarrow \text{ALD} + \text{HO}_2 + \text{OH}$	a	Scaled to J(10)
J(15)	$\text{PAA} + h\nu \rightarrow \text{CH}_3\text{O}_2 + \text{OH}$	a	Scaled to J(13)
J(16)	$\text{KET} + h\nu \rightarrow \text{ETHP} + \text{ACO}_3$	a	Scaled to J(5)

[Title Page](#)
[Abstract](#)
[Introduction](#)
[Conclusions](#)
[References](#)
[Tables](#)
[Figures](#)
[I◀](#)
[▶I](#)
[◀](#)
[▶](#)
[Back](#)
[Close](#)
[Print Version](#)
[Interactive Discussion](#)

© EGS 2001

**Clouds, HO_x and NO_x
in the MBL**

J. E. Williams et al.

Table 2. Continued...

Number	Reaction	Note	Reference
J(17)	$\text{GLY} + h\nu \rightarrow 0.13\text{HCHO} + 1.87\text{CO} + 0.87\text{H}_2$	a	Scaled to J(1)
J(18)	$\text{GLY} + h\nu \rightarrow 0.45\text{HCHO} + 1.55\text{CO} + 0.80\text{HO}_2 + 0.15\text{H}_2$	a	Scaled to J(1)
J(19)	$\text{MGLY} + h\nu \rightarrow \text{CO} + \text{HO}_2 + \text{ACO}_3$	a	Scaled to J(1)
J(20)	$\text{DCB} + h\nu \rightarrow \text{TCO}_3 + \text{HO}_2$	a	Scaled to J(10)
J(21)	$\text{ONIT} + h\nu \rightarrow 0.2\text{ALD} + 0.8\text{KET} + \text{HO}_2 + \text{NO}_2$	a	Scaled to J(5)
J(22)	$\text{MACR} + h\nu \rightarrow \text{HCHO} + \text{CO} + \text{HO}_2 + \text{ACO}_3$	a	Scaled to J(10)
J(23)	$\text{HKET} + h\nu \rightarrow \text{HCHO} + \text{HO}_2 + \text{ACO}_3$	a	Scaled to J(5)
J(24)	$\text{ClOH} + h\nu \rightarrow \text{Cl} + \text{OH}$	b	SG00
J(25)	$\text{Cl}_2\text{O}_2 + h\nu \rightarrow \text{Cl} + \text{Cl} + \text{O}_2$	b	SG00
J(26)	$\text{ClNO}_2 + h\nu \rightarrow \text{Cl} + \text{NO}_2$	b	SG00
J(27)	$\text{ClNO}_3 + h\nu \rightarrow \text{Cl} + \text{NO}_3$	b	SG00
J(28)	$\text{Cl}_2 + h\nu \rightarrow \text{Cl} + \text{Cl}$	b	SG00
J(29)	$\text{BrOH} + h\nu \rightarrow \text{Br} + \text{OH}$	b	SG00
J(30)	$\text{BrNO}_2 + h\nu \rightarrow \text{Br} + \text{NO}_2$	b	SG00
J(31)	$\text{BrNO}_3 + h\nu \rightarrow \text{Br} + \text{NO}_3$	b	SG00
J(32)	$\text{Br}_2 + h\nu \rightarrow \text{Br} + \text{Br}$	b	SG00
J(33)	$\text{BrCl} + h\nu \rightarrow \text{Br} + \text{Cl}$	b	SG00
J(34)	$\text{BrO} (+ \text{O}_2) + h\nu \rightarrow \text{Br} + \text{O}$	b	SG00

KW97: Krol and van Weele, 1997; SG00: Sander and Glasow, 2000 [a] Photolysis reactions originating from RACM chemical scheme (Stockwell et al., 1997) [b] Additional photolysis rates added to activate halogen species.

[Title Page](#)
[Abstract](#)
[Introduction](#)
[Conclusions](#)
[References](#)
[Tables](#)
[Figures](#)
[I◀](#)
[▶I](#)
[◀](#)
[▶](#)
[Back](#)
[Close](#)
[Print Version](#)
[Interactive Discussion](#)

© EGS 2001

**Clouds, HO_x and NO_x
in the MBL**

J. E. Williams et al.

Title Page

Abstract

Introduction

Conclusions

References

Tables

Figures

I◀

▶I

◀

▶

Back

Close

Print Version

Interactive Discussion

© EGS 2001

Table 3. Additional gas phase reaction rates supplemented to the RACM chemical scheme

Number	Reaction	k [molecules ⁻¹ cm ³ s ⁻¹]	Reference
G(1)	HCl + OH → Cl + H ₂ O	8.0E-13 exp(-350/T)	DM97
G(2)	Cl + O ₃ → ClO + O ₂	1.2E-11 exp(-260/T)	DM97
G(3)	Cl + CH ₄ (+ O ₂) → HCl + CH ₃ O ₂	1.0E-13 exp(-1400/T)	DM97
G(4)	Cl + HCHO (+ O ₂) → HCl + CO + HO ₂	7.3E-11 exp(-30/T)	DM97
G(5)	ClO + HO ₂ → ClOH (+ O ₂)	5.0E-12 exp(700/T)	DM97
G(6)	ClO + NO → Cl + NO ₂	1.7E-11 exp(290/T)	DM97
G(7)	ClO + NO ₂ → ClNO ₃	2.3E-12	DM97
G(8)	ClO + CH ₃ O ₂ → HCHO + Cl + HO ₂	2.2E-12 exp(-115/T)	DM97
G(9)	ClO + ClO → Cl ₂ O ₂	3.5E-13	DM97
G(10)	Cl ₂ O ₂ → ClO + ClO	49	DM97
G(11)	Cl + H ₂ O ₂ → HCl + HO ₂	4.1E-13 exp(-980/T)	DM97
G(12)	Cl + CH ₃ OOH → HCl + CH ₃ O ₂	5.7E-11	S99
G(13)	Cl + C ₂ H ₆ (+ O ₂) → HCl + ETHP	5.7E-11 exp(-90/T)	DM97
G(14)	Cl + C ₂ H ₄ (+ O ₂) → HCl + XO ₂	1.0E-10	M93
G(15)	HBr + OH → Br + H ₂ O	1.1E-11	DM97
G(16)	Br + O ₃ → BrO + O ₂	1.2E-12 exp(-800/T)	DM97
G(17)	Br + HCHO (+ O ₂) → HBr + CO + HO ₂	1.1E-12 exp(-800/T)	DM97
G(18)	BrO + HO ₂ → BrOH + O ₂	2.1E-11 exp(540/T)	DM97
G(19)	BrO + NO → Br + NO ₂	2.1E-11 exp(260/T)	DM97
G(20)	BrO + NO ₂ → BrNO ₃	2.8E-12	DM97
G(21)	BrO + CH ₃ O ₂ → HCHO + Br + HO ₂	4.1E-12	A97

**Clouds, HO_x and NO_x
in the MBL**

J. E. Williams et al.

[Title Page](#)
[Abstract](#)
[Introduction](#)
[Conclusions](#)
[References](#)
[Tables](#)
[Figures](#)
[I◀](#)
[▶I](#)
[◀](#)
[▶](#)
[Back](#)
[Close](#)
[Print Version](#)
[Interactive Discussion](#)

© EGS 2001

Table 3. Continued...

Number	Reaction	k [molecules ⁻¹ cm ³ s ⁻¹]	Reference
G(22)	BrO + CH ₃ O ₂ → BrOH + HCHO	1.6E-12	A97
G(23)	Br + CH ₃ OOH → HBr + CH ₃ O ₂	1.4E-14 exp(-1610/T)	
G(24)	Br + HO ₂ → HBr + O ₂	2.0E-12 exp(-600/T)	DM97
G(25)	Br + C ₂ H ₄ (+ O ₂) → HBr + XO ₂	2.2E-13	B93
G(26)	Cl + Br ₂ → BrCl + Br	1.2E-10	M93
G(27)	BrCl + Br → Br ₂ + Cl	3.3E-15	M93
G(28)	Cl ₂ + Br → BrCl + Cl	1.1E-15	M93
G(29)	BrCl + Cl → Cl ₂ + Br	1.5E-11	M93
G(30)	BrO + ClO → Br + ClO (+ O)	6.8E-12 exp(430/T)	DM97
G(31)	BrO + ClO → Br + Cl + O ₂	6.1E-12 exp(220/T)	DM97
G(32)	BrO + ClO → BrCl + O ₂	1.0E-12 exp(170/T)	DM97
G(33)	BrO + BrO → Br + Br + O ₂	2.7E-12 exp(40/T)	DM97
G(34)	BrO + BrO → Br ₂ + O ₂	5.0E-13 exp(860/T)	DM97
G(35)	DMS + OH → SO ₂ + HCHO + HCHO	4.4E-12 exp(-234/T)	AT92
G(36)	DMS + NO ₃ → SO ₂ + HCHO + HCHO + HNO ₃	1.1E-12 exp(520/T)	AT92
G(37)	DMS + Cl (+ O ₂) → SO ₂ + HCHO + HCHO + HCl	3.3E-10	S92
G(38)	DMS + Br (+ O ₂) → SO ₂ + HCHO + HCHO + HBr	3.0E-14 exp(-2386/T)	J94

A97: Aranda et al., 1997; AT92: Atkinson et al., 1992; B93: Barnes et al., 1993; DM97: DeMore et al., 1997; J94: Jefferson et al., 1994; M93: Mallard et al., 1993; S92: Stickel et al., 1992.

**Clouds, HO_x and NO_x
in the MBL**

 J. E. Williams et al.

[Title Page](#)
[Abstract](#)
[Introduction](#)
[Conclusions](#)
[References](#)
[Tables](#)
[Figures](#)
[I◀](#)
[▶I](#)
[◀](#)
[▶](#)
[Back](#)
[Close](#)
[Print Version](#)
[Interactive Discussion](#)

© EGS 2001

Table 4. Henry constants, mass accommodation coefficients and diffusion coefficients for HBr, ClOH, BrOH and H₂C₂O₄

Species	K [mol dm ⁻³ atm ⁻¹]	-E/R [K]	α [-]	D _g [10 ⁻⁵ m ² s ⁻¹]	reference
HBr	0.72	6077	0.05	1.0	SC96
ClOH	480	1633	0.05	1.0	SC96
BrOH	48	-	0.05	1.0	SC96
H ₂ C ₂ O ₄	5.0e8	-	0.05 ^[a]	1.0 ^[a]	SH96

[a] Estimated value SC96: Sander and Crutzen, 1996; SH96: Saxena and Hildemann, 1996.

**Clouds, HO_x and NO_x
in the MBL**

J. E. Williams et al.

Table 5. Additional aqueous phase reactions supplemented to the scheme of Herrmann et al., 2000(b)

Number	Reaction	k [M ⁻ⁿ s ⁻¹]	reference
A(1)	ClOH + Cl ⁻ + H ⁺ → Cl ₂ + H ₂ O	1.8E4	SC96
A(2)	BrOH + Br ⁻ + H ⁺ → Br ₂ + H ₂ O	1.6E10	SC96
A(3)	ClOH + Br ⁻ + H ⁺ → BrCl + H ₂ O	1.3E6	KM87
A(4)	BrOH + Cl ⁻ + H ⁺ → BrCl + H ₂ O	5.6E9	W94
A(5)	BrCl → BrOH + Cl ⁻ + H ⁺	1.0E5	W94
A(6)	BrCl + Br ⁻ → Br ₂ Cl ⁻	5.0E9	W94
A(7)	Br ₂ Cl ⁻ → BrCl + Br ⁻	2.8E5	W94
A(8)	Br ₂ + Cl ⁻ → BrCl ₂ ⁻	5.0E9	W94
A(9)	BrCl ₂ ⁻ → Br ₂ + Cl ⁻	3.9E9	W94
A(10)	Br ⁻ + ClO ⁻ + H ⁺ → BrCl + OH ⁻	3.7E10	KM87
A(11)	Br ⁻ + O ₃ (+ H ⁺) → BrO ⁻ + O ₂	2.1E2 exp(-4450/T)	HH83
A(12)	BrO ⁻ + SO ₃ ²⁻ → Br ⁻ + SO ₄ ²⁻	1.0E8	TM91
A(13)	Br ₂ ⁻ + HO ₂ → Br ₂ + H ₂ O ₂	9.1E7	WS87
A(14)	BrOH + HSO ₃ ⁻ → Br ⁻ + HSO ₄ ⁻ + H ⁺	5.0E9	(a)
A(15)	BrOH + SO ₃ ²⁻ → Br ⁻ + HSO ₄ ⁻	5.0E9	TM91
A(16)	ClOH + HSO ₃ ⁻ → Cl ⁻ + HSO ₄ ⁻ + H ⁺	7.6E8	(b)

[Title Page](#)
[Abstract](#)
[Introduction](#)
[Conclusions](#)
[References](#)
[Tables](#)
[Figures](#)
[Back](#)
[Close](#)
[Print Version](#)
[Interactive Discussion](#)

© EGS 2001

**Clouds, HO_x and NO_x
in the MBL**

J. E. Williams et al.

Table 5. Continued...

Number	Reaction	k [M ⁻ⁿ s ⁻¹]	reference
A(17)	ClOH + SO ₃ ²⁻ → Cl ⁻ + HSO ₄ ⁻	7.6E8	F89
A(18)	Br ⁻ + HSO ₅ ⁻ → BrOH + SO ₄ ²⁻	1.0 exp(-5338/T)	F60
A(19)	Cl ⁻ + HSO ₅ ⁻ → ClOH + SO ₄ ²⁻	1.8E-2 exp(-7352/T)	F60
A(20)	HBr → H ⁺ + Br ⁻	1.0E13	L69
A(21)	H ⁺ + Br ⁻ → HBr	1.0E4	L69
A(22)	ClOH → H ⁺ + ClO ⁻	3.2E2	L69
A(23)	H ⁺ + ClO ⁻ → ClOH	1.0E10	L69
A(24)	BrOH → H ⁺ + BrO ⁻	23	KT56
A(25)	H ⁺ + BrO ⁻ → BrOH	1.0E10	KT56

(a) A(14) estimated to be equal to A(15), (b) A(16) estimated to be equal to A(17) F89: Fogelman et al., 1989; F60: Fortnum et al., 1960; HH83: Haag and Hoigne, 1983; KM87: Kumar and Margerum, 1987; KT56: Kelley and Tartar, 1956; L69: Lax, 1969; TM91: Troy and Mergerum, 1991; WS87 Wagner and Strehlow, 1987; W94: Wang et al., 1994.

Title Page

Abstract

Introduction

Conclusions

References

Tables

Figures

I◀

▶I

◀

▶

Back

Close

Print Version

Interactive Discussion

© EGS 2001

Table 6. Initial trace gas concentrations used for 1-D model simulations. For definitions of the abbreviations for chemical species the reader is referred to Stockwell et al., 1997

Species	C _o ppbv	reference	Species	C _o ppbv	reference
NO ₂	0.1	(E)	ORA2	0	(E)
HNO ₃	0.15	J86	OLT	0	(E)
CH ₄	1700	ZP96	ISO	0	(E)
H ₂ O ₂	1	Z98	TOL	0	ZP96
H ₂	500	(E)	CSL	0	ZP96
NH ₃	0.5	(E)	XYL	0	ZP96
CO	140	(E)	ALD	0.01	ZP96
O ₃	30	(E)	Ketones	0.1	(E)
HCl	0.5	Z98	GLY	0.01	ZP96
CO ₂	3.3e5	GW81	MGLY	0.01	ZP96
SO ₂	0.1	K00	PAN	0	(E)
HCHO	0.5	(E)	OP1	1	(E)
ETH	0.5	ZP96	OP2	0.1	(E)
HC ₃	1	ZP96	PAA	0.001	ZP96
HC ₅	0	ZP96	CH ₃ OH	0.5	(E)
HC ₈	0	ZP96	EtOH	0	(E)
C ₂ H ₄	0.1	ZP96	API	0	(E)
ORA1	0.25	B00	LIM	0	(E)
DMS	0.11	(E)			

(E) symbolises an estimated value B00: Barboukas, 2000; GW81: Graedel and Weschler, 1981; J86: Jacob, 1986; K00: Krische et al., 2000; Z98 : Zhang et al., 1998; ZP Zimmerman and Poppe, 1996.

Clouds, HO_x and NO_x in the MBL

J. E. Williams et al.

Title Page

Abstract

Introduction

Conclusions

References

Tables

Figures

◀

▶

◀

▶

Back

Close

Print Version

Interactive Discussion

© EGS 2001

**Clouds, HO_x and NO_x
in the MBL**

J. E. Williams et al.

Table 7. Emission fluxes incorporated into the 1-D model

Species	J_e (Marine) $\text{cm}^{-2} \text{s}^{-1}$	Reference
O ₃	5.0e10	SC96
NH ₃	2.0e9	SC96
DMS	2.0e9	SC96
CO	2.0e10	SC96
NO	2.5e8	SC96
ETH	3.6e7	P95
ETE	1.8e8	P95
CH ₃ SCH ₃	2.0e9	SC96

SC96: Sander and Crutzen, 1996; P95: Plass-Dulmer et al., 1995.

[Title Page](#)[Abstract](#)[Introduction](#)[Conclusions](#)[References](#)[Tables](#)[Figures](#)[I◀](#)[▶I](#)[◀](#)[▶](#)[Back](#)[Close](#)[Print Version](#)[Interactive Discussion](#)

© EGS 2001

**Clouds, HO_x and NO_x
in the MBL**

J. E. Williams et al.

Table 8. Deposition velocities incorporated into the 1-D model

Species	ν_d cm s ⁻¹
O ₃	0.04
NH ₃	1.0
CO	0.1
SO ₂	0.5
NO ₂	0.1
HCl	0.5
H ₂ SO ₄	0.5
HNO ₃	0.5
HCHO	0.5
OP1	0.5
ORA1	0.5
CH ₃ OH	0.5
EtOH	0.5

[Title Page](#)[Abstract](#)[Introduction](#)[Conclusions](#)[References](#)[Tables](#)[Figures](#)[I◀](#)[▶I](#)[◀](#)[▶](#)[Back](#)[Close](#)[Print Version](#)[Interactive Discussion](#)

© EGS 2001

**Clouds, HO_x and NO_x
in the MBL**

J. E. Williams et al.

Title Page

Abstract

Introduction

Conclusions

References

Tables

Figures

◀

▶

◀

▶

Back

Close

Print Version

Interactive Discussion

© EGS 2001

Table 9. Key to 1-D simulations performed to investigate the effect of cloud on gas phase species

Simulation No.	Details of the simulation
I	Clear Sky gas phase run only
II	Attenuated gas phase run only
III	Gas and Cloud chemistry only
IV	Gas, Cloud and Aerosol run
V	As for III except HNO ₄ and HONO phase transfer is ignored and eqbm (13) inactive
VI	As for III except NO ₃ ⁻ photolysis turned off
VII	As for III except halogen reactions turned off

Clouds, HO_x and NO_x in the MBL

J. E. Williams et al.

Table 10. a Ratios between simulations (III) / (I) (in paranthesis) and (III) / (I)

Gaseous Species	Overall average		Height		Height		Above Boundary Layer	
	0–2000 m		<600 m	600–1520 m		>1520 m		
O ₃	(0.96)	0.98	(0.97)	0.98	(0.96)	0.98	(0.96)	1.00
H ₂ O ₂	(0.75)	0.71	(0.90)	0.91	(0.44)	0.41	(1.23)	1.00
OH	(0.87)	0.98	(0.38)	1.10	(0.90)	0.85	(2.23)	1.00
HO ₂	(0.64)	0.76	(0.55)	1.02	(0.42)	0.42	(1.54)	1.00
NO	(1.49)	1.74	(0.76)	1.50	(2.21)	2.22	(1.51)	1.00
NO ₂	(1.89)	1.61	(2.03)	1.47	(2.11)	1.94	(0.79)	1.00
HONO	(67.10)	61.89	(73.61)	74.45	(82.45)	69.64	(1.52)	1.00
HNO ₄	(1.07)	1.19	(1.24)	1.65	(0.85)	0.79	(1.21)	1.00
PAN	(0.92)	1.02	(0.96)	1.05	(0.91)	0.99	(0.81)	1.00

[Title Page](#)
[Abstract](#)
[Introduction](#)
[Conclusions](#)
[References](#)
[Tables](#)
[Figures](#)
[Back](#)
[Close](#)
[Print Version](#)
[Interactive Discussion](#)

© EGS 2001

Clouds, HO_x and NO_x in the MBL

J. E. Williams et al.

Table 10. b Ratios between simulations (III) / (I) (in paranthesis) and (IV) / (I)

Gaseous Species	Overall average		Height		Height		Above Boundary Layer	
	0–2000 m		<600 m		600–1520 m		>1520 m	
O ₃	(0.95)	0.96	(0.95)	0.96	(0.94)	0.96	(0.96)	1.00
H ₂ O ₂	(0.65)	0.62	(0.75)	0.76	(0.36)	0.34	(1.23)	1.00
OH	(0.86)	0.94	(0.35)	1.00	(0.91)	0.87	(2.23)	1.00
HO ₂	(0.64)	0.75	(0.50)	0.93	(0.47)	0.49	(1.54)	1.00
NO	(1.42)	1.64	(0.70)	1.39	(2.12)	2.11	(1.51)	1.00
NO ₂	(1.76)	1.51	(1.86)	1.35	(2.00)	1.84	(0.79)	1.00
HONO	(64.22)	58.63	(64.41)	64.49	(84.91)	71.98	(1.52)	1.00
HNO ₄	(0.96)	1.04	(0.94)	1.25	(0.90)	0.84	(1.21)	1.00
PAN	(0.74)	0.82	(0.68)	0.74	(0.78)	0.85	(0.81)	1.00

Title Page

Abstract

Introduction

Conclusions

References

Tables

Figures

◀

▶

◀

▶

Back

Close

Print Version

Interactive Discussion

© EGS 2001

**Clouds, HO_x and NO_x
in the MBL**

 J. E. Williams et al.

Table 11. Ratios between run V/I to highlight the effect of that heterogeneous conversion of NO₂ to NO has on [HO_x]_g.and [NO_x]_g

Species	Overall average	Height		
		<600 m	600–1520 m	Above Boundary Layer >1520 m
O ₃	0.95	0.95	0.94	0.96
H ₂ O ₂	0.74	0.89	0.43	1.23
OH	0.77	0.34	0.72	2.23
HO ₂	0.61	0.51	0.39	1.54
NO	0.91	0.49	1.13	1.51
NO ₂	1.21	1.30	1.25	0.79
HONO	0.99	0.78	1.02	1.52
HNO ₄	0.64	0.66	0.43	1.21
PAN	0.65	0.65	0.58	0.81

[Title Page](#)
[Abstract](#)
[Introduction](#)
[Conclusions](#)
[References](#)
[Tables](#)
[Figures](#)
[I◀](#)
[▶I](#)
[◀](#)
[▶](#)
[Back](#)
[Close](#)
[Print Version](#)
[Interactive Discussion](#)

© EGS 2001

**Clouds, HO_x and NO_x
in the MBL**

 J. E. Williams et al.

Table 12. Differences in the ratios of (NO/(NO+ NO₂)) for cases (I – VI) to show the effect of aqueous phase HNO₄ chemistry on NO_{x(g)}

Case No.	Overall average	Height	Height	Above Boundary Layer
		<600 m	600–1520 m	>1520 m
(I)	0.331	0.309	0.344	0.353
(II)	0.262	0.144	0.300	0.504
(III)	0.277	0.146	0.332	0.504
(IV)	0.278	0.147	0.332	0.504
(V)	0.275	0.149	0.326	0.504
(VI)	0.275	0.149	0.326	0.504

[Title Page](#)
[Abstract](#)
[Introduction](#)
[Conclusions](#)
[References](#)
[Tables](#)
[Figures](#)
[I◀](#)
[▶I](#)
[◀](#)
[▶](#)
[Back](#)
[Close](#)
[Print Version](#)
[Interactive Discussion](#)

© EGS 2001

**Clouds, HO_x and NO_x
in the MBL**

J. E. Williams et al.

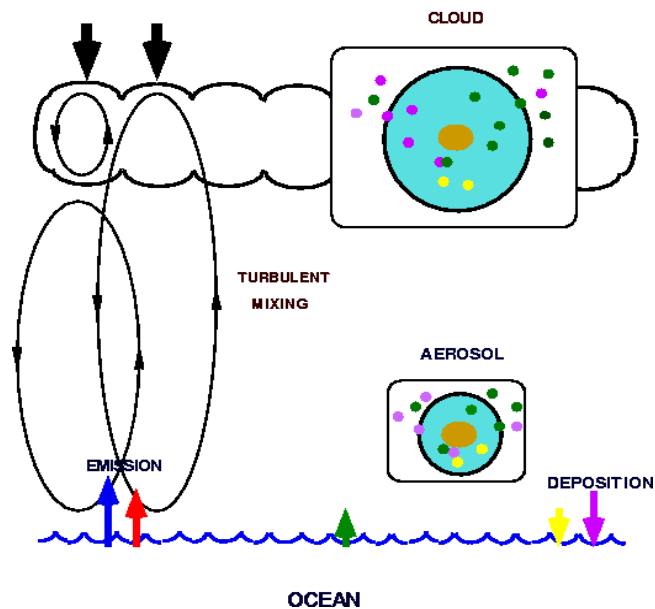


Fig. 1. Schematic representation of the 1-D stratocumulus cloud model of van den Berg et al. (2000) for the simulation of the chemical and physical processes which occur in the Marine Boundary Layer.

[Title Page](#)[Abstract](#)[Introduction](#)[Conclusions](#)[References](#)[Tables](#)[Figures](#)[◀](#)[▶](#)[◀](#)[▶](#)[Back](#)[Close](#)[Print Version](#)[Interactive Discussion](#)

© EGS 2001

**Clouds, HO_x and NO_x
in the MBL**

J. E. Williams et al.

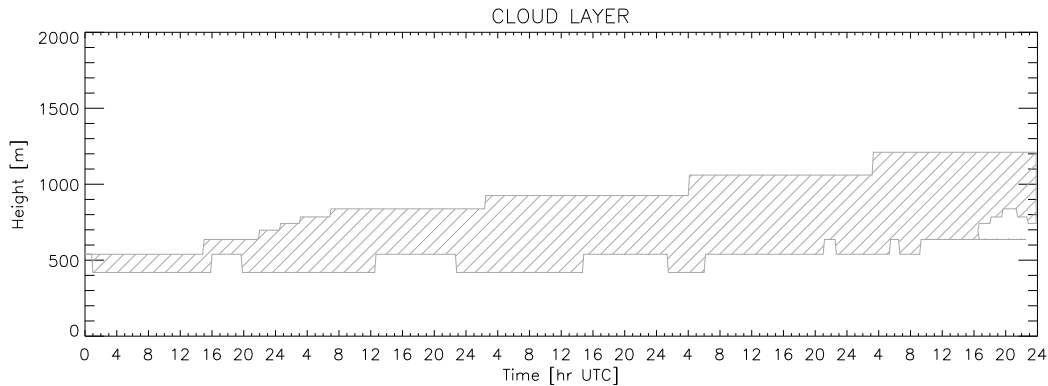


Fig. 2. Development of the cloud layer in the 1-D stratocumulus cloud model over a 5-day simulation. The cloud layer is symbolised by the shaded region.

[Title Page](#)[Abstract](#)[Introduction](#)[Conclusions](#)[References](#)[Tables](#)[Figures](#)[◀](#)[▶](#)[◀](#)[▶](#)[Back](#)[Close](#)[Print Version](#)[Interactive Discussion](#)

© EGS 2001

Clouds, HO_x and NO_x
in the MBL

J. E. Williams et al.

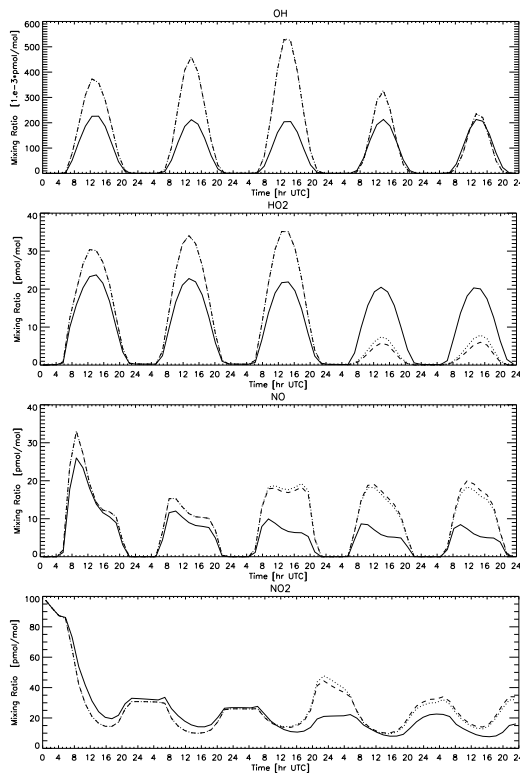


Fig. 3. Comparison of $[\text{HO}_x]_g$ and $[\text{NO}_x]_g$ species at 1060 m above sea-level over a 5-day simulation to show the differences introduced by cloud and aerosol/cloud interactions. The reader is referred to diagram 2 regarding development of the cloud layer. (—) case (I), (---) case (III), and (···) case (IV).

[Title Page](#)[Abstract](#)[Introduction](#)[Conclusions](#)[References](#)[Tables](#)[Figures](#)[◀](#)[▶](#)[◀](#)[▶](#)[Back](#)[Close](#)[Print Version](#)[Interactive Discussion](#)

© EGS 2001

Clouds, HO_x and NO_x
in the MBL

J. E. Williams et al.

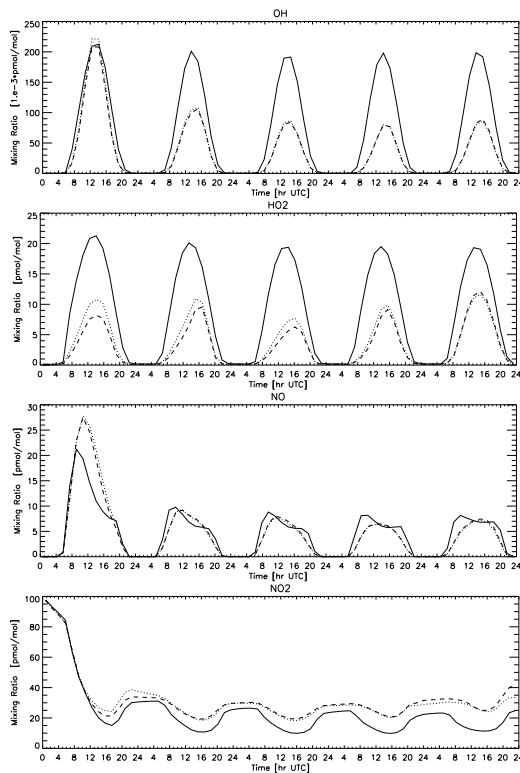


Fig. 4. Comparison of $[\text{HO}_x]_g$ and $[\text{NO}_x]_g$ species at 540 m above sea-level over a 5-day simulation to show the differences introduced by cloud and aerosol/cloud interactions. The reader is referred to diagram 2 regarding development of the cloud layer. (—) case (I), (---) case (III), and (⋯) case (IV).

[Title Page](#)[Abstract](#)[Introduction](#)[Conclusions](#)[References](#)[Tables](#)[Figures](#)[◀](#)[▶](#)[◀](#)[▶](#)[Back](#)[Close](#)[Print Version](#)[Interactive Discussion](#)

© EGS 2001

**Clouds, HO_x and NO_x
in the MBL**

 J. E. Williams et al.

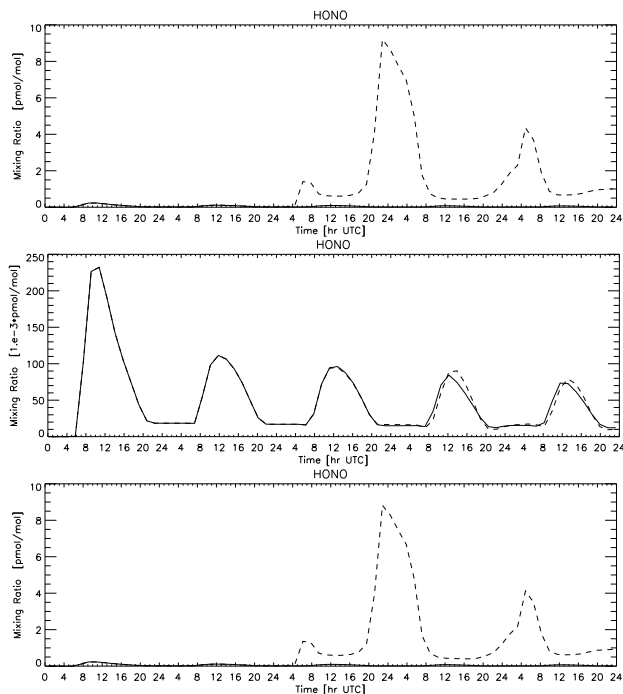


Fig. 5. Comparison of $[\text{HONO}]_g$ at 1060 m above sea-level for a 5 day simulation. The reader is referred to diagram 2 regarding development of the cloud layer. (—) $[\text{HONO}]_g$ profile for case (II) (---) $[\text{HONO}]_g$ profile for (a) case (III), (b) case (V) and (c) case (VI)

[Title Page](#)
[Abstract](#)
[Introduction](#)
[Conclusions](#)
[References](#)
[Tables](#)
[Figures](#)
[I◀](#)
[▶I](#)
[◀](#)
[▶](#)
[Back](#)
[Close](#)
[Print Version](#)
[Interactive Discussion](#)

© EGS 2001

**Clouds, HO_x and NO_x
in the MBL**

 J. E. Williams et al.

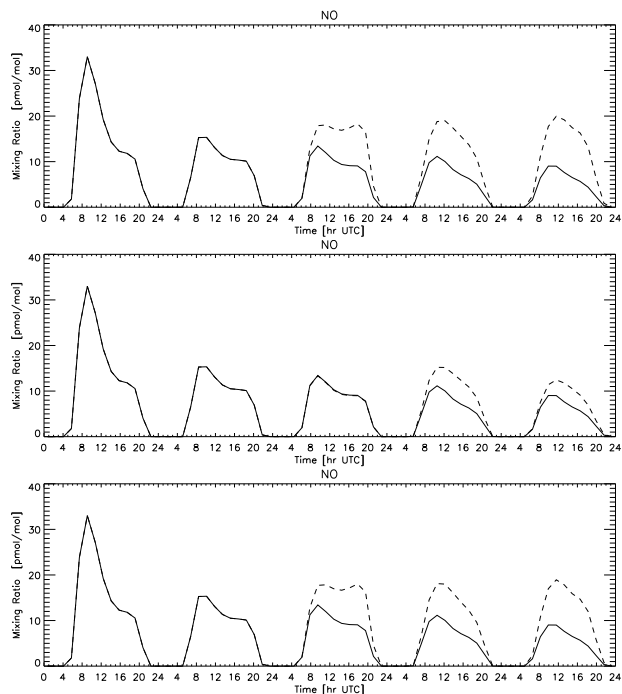


Fig. 6. Comparison of $[\text{NO}]_g$ at 1060 m above sea-level for a 5 day simulation. The reader is referred to diagram 2 regarding development of the cloud layer. (—) $[\text{NO}]_g$ profile for case (II) (---) $[\text{NO}]_g$ profile for (a) case (III), (b) case (V) and (c) case (VI)

[Title Page](#)
[Abstract](#)
[Introduction](#)
[Conclusions](#)
[References](#)
[Tables](#)
[Figures](#)
[I◀](#)
[▶I](#)
[◀](#)
[▶](#)
[Back](#)
[Close](#)
[Print Version](#)
[Interactive Discussion](#)

© EGS 2001

Clouds, HO_x and NO_x
in the MBL

J. E. Williams et al.

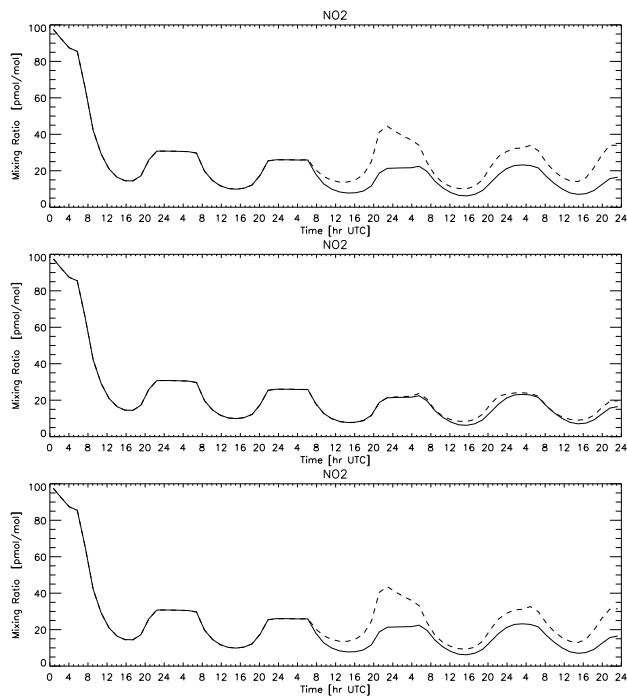


Fig. 7. Comparison of $[\text{NO}_2]_g$ at 1060 m above sea-level for a 5 day simulation. The reader is referred to diagram 2 regarding development of the cloud layer. (—) $[\text{NO}_2]_g$ profile for case (II) (---) $[\text{NO}_2]_g$ profile for (a) case (III), (b) case (V) and (c) case (VI).

[Title Page](#)[Abstract](#)[Introduction](#)[Conclusions](#)[References](#)[Tables](#)[Figures](#)[◀](#)[▶](#)[◀](#)[▶](#)[Back](#)[Close](#)[Print Version](#)[Interactive Discussion](#)

© EGS 2001